Journal of Medicinal Chemistry

Article

Synthesis and Pharmacological Evaluation of Noscapine Inspired 5-Substituted Tetrahydroisoquinolines as Cytotoxic Agents

Shane M. Devine, Cassandra Yong, Dzifa Amenuvegbe, Luigi Aurelio, Divya muthiah, Colin W. Pouton, Richard Callaghan, Ben Capuano, and Peter J. Scammells

J. Med. Chem., **Just Accepted Manuscript** • DOI: 10.1021/acs.jmedchem.8b00986 • Publication Date (Web): 29 Aug 2018

ACS Publications

is published by the American Chemical Society. 1155 Sixteenth Street N.W., Washington, DC 20036

Synthesis and Pharmacological Evaluation of Noscapine-Inspired 5-Substituted Tetrahydroisoquinolines as Cytotoxic Agents

Shane M. Devine,[†] Cassandra Yong,[†] Dzifa Amenuvegbe,[‡] Luigi Aurelio,[†] Divya Muthiah,[‡] Colin Pouton,[§] Richard Callaghan,[‡] Ben Capuano,[†] Peter J. Scammells[†,*]

[†] *Medicinal Chemistry and* [§] *Drug Delivery, Disposition and Dynamics, Monash Institute of Pharmaceutical Sciences; Monash University, Parkville, VIC 3052, Australia*

[‡] *Research School of Biology, Australian National University, Canberra, ACT 0200, Australia*

ABSTRACT: A series of 5-substituted tetrahydroisoquinolines was synthesised via a 10-step linear synthesis to assess whether replacement of noscapine's southern isobenzofuranone with other moieties retained cytotoxic activity. One such molecule, **18g** bearing a *para*-methoxybenzyl functionality with *N*-ethylcarbamoyl substitution produced cell cycle arrest at the G2/M phase with an EC_{50} of 2.7 μM in the MCF-7 breast cancer cell line; a 7-fold increase compared with noscapine (**5**). This molecule had similar activity (EC_{50} of 2.5 μM) against the resistant NCI/Adr^{RES} cell line, demonstrating its potential to overcome or avert known resistance mechanisms, unlike current cytotoxic agents. Compound **18g** was found to modify the drug efflux activity of P-gp and in combination studies, potentiate the antiproliferative activity of vinblastine. These results provide insights into the structural modifications to noscapine that will guide future development towards more potent cytotoxic agents that are active at resistant cancer cells.

■ INTRODUCTION

Tubulin targeting compounds have been, and continue to be, of major importance in cancer chemotherapy. Compounds acting on tubulin disrupt microtubule dynamics; these microtubules are cytoskeletal fibres crucial throughout the cell cycle, especially in the mitotic phase. Tubulin-disrupting agents fall into two classes; namely tubulin-polymerisation inhibitors (TPIs) and tubulin-depolymerisation inhibitors (TDIs). There are many classes of molecules that act via these two mechanisms and these have historically been derived from natural products. Examples of TPIs include vinca alkaloids, such as vincristine (**1**) and colchicine (**2**), whereas taxanes, such as paclitaxel (**3**) and epothilones, including epothilone B (**4**) act as TDIs (Figure 1). Although these agents have found great utility as anticancer agents and significantly decreased the burden of cancer on human society, their efficacy is limited *in vivo* due to numerous toxic side effects and multiple resistance mechanisms. Another example of a TPI is that of noscapine (**5**), the motivation of this current work.

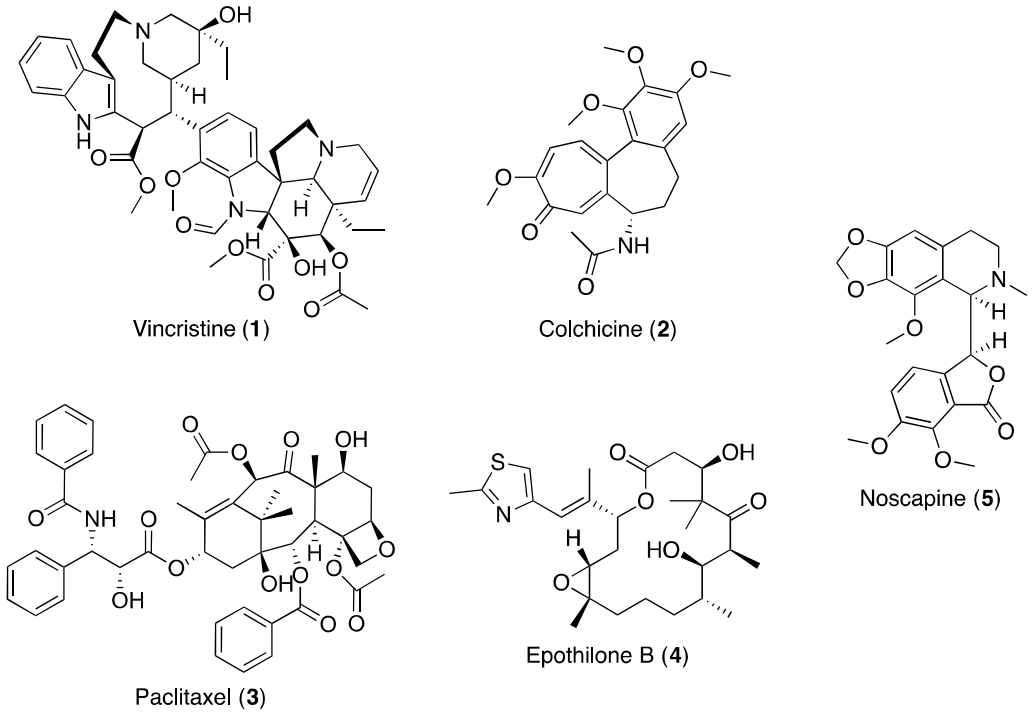

Figure 1. Examples of tubulin disrupting agents **1**–**5**.

Noscapine is a phthalideisoquinoline alkaloid isolated from the opium poppy, *Papaver somniferum* constituting approximately 1-10% of the alkaloid content of the poppy. Noscapine's initial indication was as an antitussive agent since the discovery of its cough suppressing abilities.[1,2] It is orally administered with a measured absolute oral bioavailability of 30%,[3] and a half-life of 4.5 hours.[4] It has been used clinically since the 1950s, demonstrating its good safety and pharmacokinetic profile. Unlike morphine and codeine, noscapine does not exhibit addictive, analgesic and sedative traits indicating action at a distinctly separate receptor to that of the opiate receptors.[2] In 1998, Ye et al. demonstrated that noscapine could arrest cells at mitosis, induce apoptosis, act on tubulin to impair microtubule dynamics and shrink tumours in vivo.[5] Noscapine's cytotoxic activity was relatively weak measured against cervical (HeLa), breast (MCF-7) and bladder (Renal 1983) cancer cell lines with IC_{50} values of 25 μM, 42 μM and 39 μM, respectively. The structures of noscapine and colchicine are seemingly similar, consisting of poly-oxygenated ring systems with electron-donating methoxy groups and bridged by a saturated ring. However, competition binding experiments with [^{3}H]colchicine/noscapine indicate that noscapine acts at a different binding site on tubulin, compared with colchicine.[5] Experimental and computational insights revealed noscapine to bind tubulin at either a partially overlapping site to colchicine or a distinctly non-overlapping sight that does not interfere with colchicine binding to tubulin.[6-10] Notably, there is no evidence to suggest that noscapine can bind the vinca alkaloid site. Acting as a TPI, noscapine arrests cells at the G2/M phase, whereby the cell remains in a prometaphase/metaphase-like state, which subsequently elicits apoptosis. Many groups have demonstrated noscapine's potential as an anticancer agent both *in vitro* and *in vivo* over the last two decades.[11-18] Our work aims to better define the structural changes that can be incorporated to enhance this anticancer activity.

Modification of the noscapine scaffold has been of considerable interest in the intervening years, with changes occurring primarily at the 1, 7, 6′- and 9′-positions.[16,19] The deployment of halogens at the 9′-position gave better activity in the order of 2-fold magnitude.[20] It was also demonstrated that the potentially deleterious lactone moiety at the 1-position could be replaced with a cyclic ether, as

exemplified by 9′-chloronoscapine derivative **6** (Figure 2), which retained activity.[20] Anderson et al. established a method to selectively demethylate at the 7-position using MeMgBr and BnOH to afford the corresponding phenol (**7**).[21] This approach afforded O-substituted products, which exhibited an S-phase arresting phenotype, as well as 7-amino containing moieties. The 7-hydroxy and 7-amino containing noscapinoids were shown to be G2/M phase arresting molecules that exhibit approximately 500-fold increased potency compared to noscapine (**5**).[22] These compounds also demonstrated good oral bioavailability in mice. In particular, the aniline **8** exhibited an IC_{50} of 94 nM in SNU398 cells. Further work detailed tubulin-binding experiments by STD NMR demonstrating the aniline to have a similar binding site to that of colchicine. Unfortunately though, this molecule suffered from high *in vivo* clearance in rats.[23] Our group has strived to further these contributions to enhance the activity of noscapine's cytotoxic activity and generate a more global picture of the structure-activity relationship (SAR). The combination of *N*-substitution reactions, coupled with lactone removal resulted in a series of 6′-substituted noscapinoids of which the 6′-ethylcarbonyl containing analogue **9** was the most promising.[24] This analogue exhibited EC_{50} values of 6.7 μM and 3.6 μM for the prostate (PC3) and breast (MCF-7) cancer cell lines, respectively. This was enhanced with the added benefits of 9′-halogen insertion and 7-demethylation, with the 9′-chloro–cyclic ether analogue **10** displaying EC_{50} values of 1.5, 1.7 and 0.9 μM for the prostate (PC3), breast (MCF-7) and pancreatic (PANC-1) cell lines, respectively.[25]

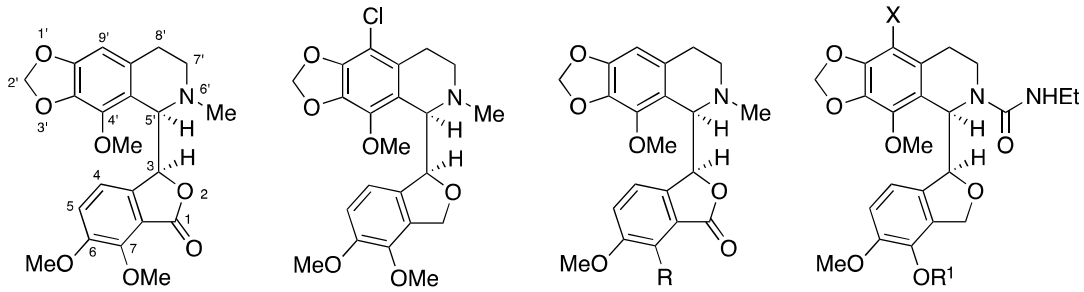

Figure 2. Key modifications made to noscapine to map structure-activity relationships.

Importantly, this molecule and similar noscapinoids demonstrate comparable efficacy against sensitive and resistant breast cancer cell lines, indicating their inability to act as substrates for efflux transporter pumps ABCB1 and ABCG2.[25] This is contrasted with known potent cytotoxic agents such as mitoxantrone and vinblastine exhibiting marked differences between these cell lines, with reductions of 17-fold and 260-fold differences, respectively. Clearly, the promise of a more potent noscapine analogue with these features will be of broad significance to the field as a novel cytotoxic agent with lower susceptibility to resistance mediators.

One aspect of noscapine's structure that could be deleterious *in vivo* is that of the lactone on the southern heterocycle. Zimmermann and co-workers showed that removal of the southern isobenzofuranone and replacement with various alkynes could retain activity similar to that of noscapine. This series of novel molecules was made possible by Bischler-Napieralski cyclization of readily accessible carbamates to the corresponding 3,4-dihydroisoquinolin-1(*2H*)-ones generating the appropriate tetrahydroisoquinoline (THIQ) scaffold. Many compounds were inactive, however one featuring a (*m*-methoxyphenyl)ethynyl group (**11**) exhibited greater inhibition of mitosis and a higher antiproliferative activity (Figure 3).[26] Crucially, it exhibited similar activity against multidrug-resistant HeLa KB-V1 cell line, which expresses the multidrug efflux pump P-glycoprotein (P-gp).

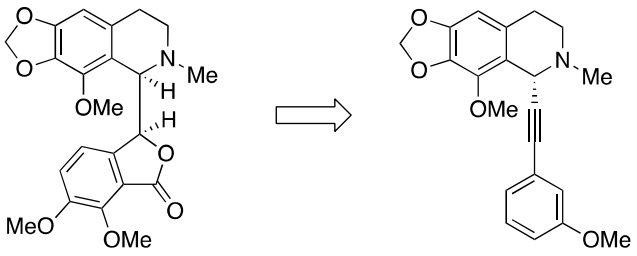

Figure 3. Southern heterocycle replacement retains activity.[26]

With these historical changes in mind, we sought to exploit modifications to the southern heterocycle to enhance activity via a linear route. These changes would incorporate aromatic rings containing electron-donating methoxy groups with mono-, di- or tri-substitution patterns. These modifications would demonstrate the smallest deviation from noscapine's structure, whilst hopefully

maintaining activity. Our *N*-ethylcarbamoyl group was also incorporated for anticipated higher potency gains.

■ RESULTS AND DISCUSSION

Chemistry. To generate our target 5-substituted noscapinoid molecules we envisaged a linear route which included a Bischler-Napieralski cyclisation[27] to generate the tetrahydroisoquinoline scaffold. Firstly, selective bromination of vanillin (**12**) afforded 5-bromovanillin in excellent yield (Scheme S1, Supporting Information). This was then subjected to a copper-mediated hydroxylation to form a catechol. Selective bromination once again was employed and further cyclisation with diiodomethane generated the precursor dioxole. The incorporation of the bromine atom was important for two reasons. Firstly, halogens in this position of noscapine engender better activity. Secondly, under the following dehydrative Bischler-Napieralski conditions with this position unoccupied, inseparable mixtures of tricyclic products ensued (unpublished work). A nitro-aldol reaction with nitromethane formed the nitro-alkene and subsequent reduction with borane produced the key intermediate, namely arylethanamine (**13**). The borane was necessary as the reducing agent as other standard methods also removed the bromine atom. Unfortunately, a significant amount of hydroxylamine by-product was also formed, similar to that described by Guy et al.[28] Pleasingly, sufficient material was obtained to complete the synthesis. Reaction with an appropriate benzoic acid via EDCI/HOBt amide coupling conditions generated the diversity in our series, the amides (**14**) (Scheme 1). Installation of various benzoic and phenylacetic acids containing mono, di or trimethoxy groups furnished the coverage of potential SAR assessment to address the suitability of the southern heterocycles removal. The choice of electron-donating methoxy groups was selected to give comparable information to that of previously identified noscapinoid and THIQ compounds. Bischler-Napieralski cyclisation with $POCl_3$ generated the dihydroisoquinolines (**15**), which were directly reduced with $NaBH_4$ to the tetrahydroisoquinolines (**16**). Finally, *N*-substitution was undertaken with a methylating agent (MeI or CH_2O) or ethyl isocyanate to give the N^6-substituted compounds **17** and **18**, respectively. MeI was initially used for the alkylation, however this reaction

suffered from poor yields (12–37%) due to the fact that unwanted quaternized material formed preferentially.

Scheme 1. Synthesis of 5-substituted noscapinoids[a]

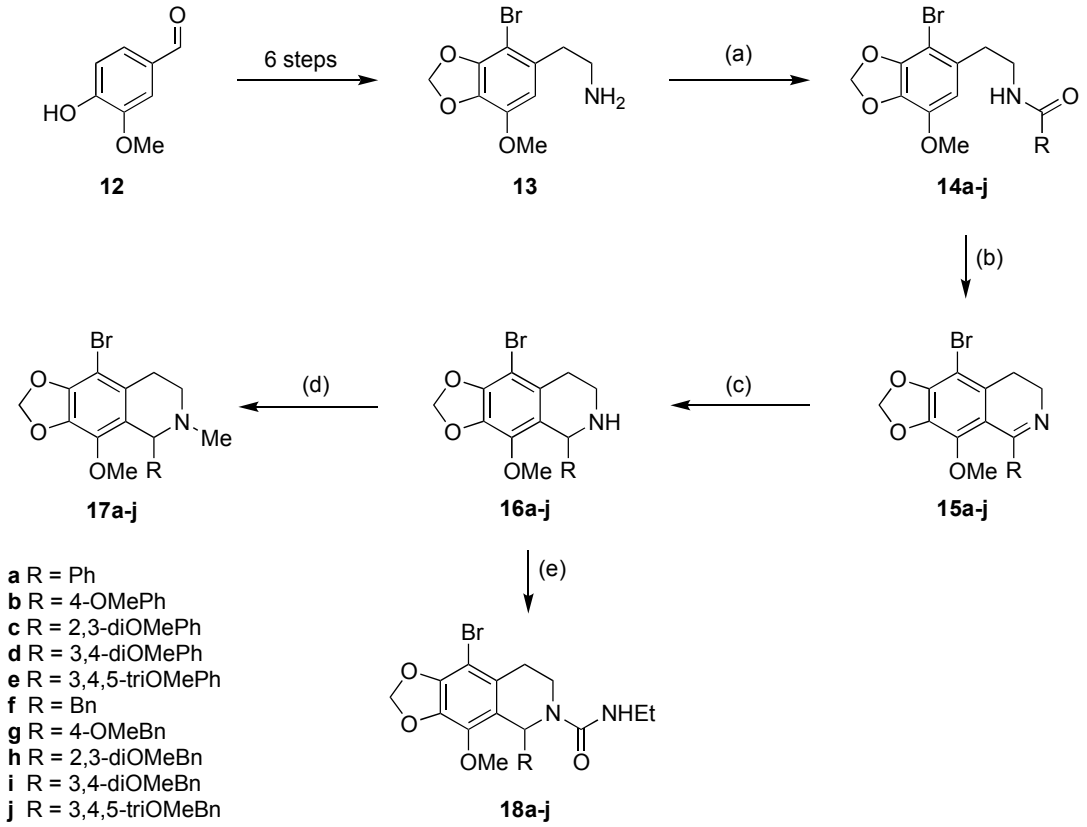

[a]Reagents and conditions: (a) R-CO_2H, HOBt, EDCI, DIPEA, 25 °C, 16 h, 87–98%; (b) $POCl_3$, PhMe, 120 °C, 2 h, 86–99%; (c) $NaBH_4$, MeOH, -78 °C, 30 min, 47–94%; (d) i) MeI, K_2CO_3, DMF, 25 °C, 3 h, for **17a**, **c**, **f**, **g**, **h**, **i**, **j**, 12–37%; ii) HCOOH, CH_2O, 80 °C, 2 h, for (**17b, d, e**), 83–85%; (e) EtNCO, MeCN, 0 °C, 1 h, 62–93%.

Compounds **17b**, **17d** and **17e** were synthesised by an alternative method using CH_2O in formic acid as the methyl source. Under these conditions, when 2-(2,3-dimethoxyphenyl)acetic acid was installed as for **16h**, an unexpected result ensued. The ^{1}H NMR spectrum of the isolated compound lacked the *N*-methyl signal (usually present at ~2.3 ppm), the disappearance of an aromatic proton and the presence of an additional methylene signal, corresponding to the berberine-like structure **19** (Scheme 2). This was confirmed by 2D NMR spectroscopy. Ring cyclisation affording berberine-

like entities in the presence of formic acid and formaldehyde have been previously described by Sun et al.[29] We speculate that the formation of this berberine-like compound takes place through formaldehyde insertion, an iminium intermediate and subsequent cyclisation.

Scheme 2. Synthesis of the berberine analogue 19[a]

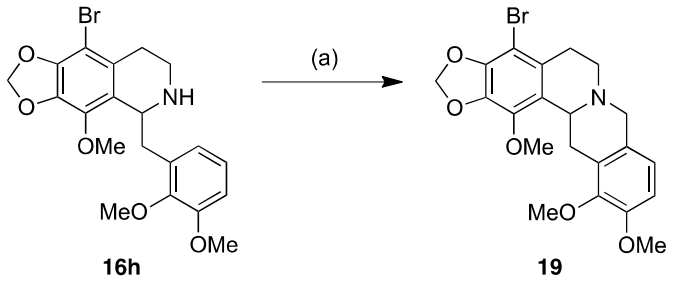

16h **19**

[a]Reagents and conditions: (a) HCOOH, CH_2O, 80 °C, 2 h, 47%.

Pharmacology. *Cell cycle arrest assays.* Cell cycle arrest assays provided preliminary evaluation to assess the ability of novel 5-substituted THIQs to cause advanced G2/M phase arrest through disruption of microtubule assembly (Table 1). Cells were stained with Hoechst 33342 following 18 h treatment with positive controls, vincristine (100 nM), noscapine (**5**) (10 μM) or test compounds **17a–j**, **18a–j** and **19** (10 μM) and analysed with FACSCanto II fluorescence-activated cell sorting (FACS) analyser. The percentage of cells present at three stages of the cell proliferation cycle (G1, S and G2/M) was obtained following data processing with FlowJo (v10). The percentage increase in G2/M arrest was calculated with reference to the vehicle control (0.1% DMSO).

The standout compounds based on the cell cycle arrest data were the 5-(4-methoxybenzyl)-substituted THIQs **17g** and **18g**, both of which produced significantly greater increases in G2/M arrest than noscapine (**5**) in MCF-7 and PANC-1 cells. For example, **18g** produced a 208% increase in G2/M arrest in MCF-7 cells and a 175% increase in PANC-1 cells, relative to the 2% and 16% increases observed for **5**. The 4-methoxy group was clearly a key contributor to the target binding interactions as the compounds which lacked this moiety / possessed an unsubstituted benzyl in the 5-position exhibited a minimal percentage increase in G2/M arrest (0–13%). Furthermore, the

presence of more than one methoxy group in compounds **17h–j** and **18h–j** also led to a reduction in activity relative to **17g** and **18g**, with moderate G2/M arrest of 0-32% across the two cell lines. The berberine-like THIQ derivative **19** showed 28% and 9% increase in G2/M arrest with reference to the control, in MCF-7 and PANC-1 cells, respectively.

Table 1. Percentage increase in arrested cells trapped in the G2/M phase for THIQs 17a-j, 18a-j and 19.

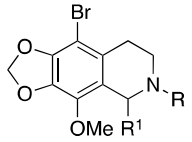

Cpd	Structural Modifications		% Increase in G2/M Arrest[a]	
	R	**R[1]**	**MCF-7**	**PANC-1**
Vincristine[b]	-	-	283 ± 15	265 ± 12
5	-	-	2 ± 0.4	16 ± 4.0
17a	Me	Ph	18 ± 4.4	-7 ± 7.5
17b	Me	4-OMePh	23 ± 7.6	26 ± 6.9
17c	Me	2,3-diOMePh	29 ± 7.7	16 ± 7.6
17d	Me	3,4-diOMePh	20 ± 6.7	8 ± 14
17e	Me	3,4,5-triOMePh	48 ± 24	12 ± 5.0
17f	Me	Bn	9 ± 3.4	13 ± 12
17g	Me	4-OMeBn	180 ± 23	226 ± 44
17h	Me	2,3-diOMeBn	32 ± 5.8	8 ± 12
17i	Me	3,4-diOMeBn	19 ± 4.0	0 ± 8.6
17j	Me	3,4,5-triOMeBn	-8 ± 1.7	-1 ± 7.5
18a	C(O)NHEt	Ph	6 ± 1.9	-2 ± 2.8
18b	C(O)NHEt	4-OMePh	18 ± 2.7	21 ± 5.6
18c	C(O)NHEt	2,3-diOMePh	19 ± 12	14 ± 1.4
18d	C(O)NHEt	3,4-diOMePh	-6 ± 2.6	11 ± 6.5
18e	C(O)NHEt	3,4,5-triOMePh	3 ± 0.3	2 ± 2.8
18f	C(O)NHEt	Bn	1 ± 3.0	-8 ± 8.8
18g	C(O)NHEt	4-OMeBn	208 ± 7.2	175 ± 37
18h	C(O)NHEt	2,3-diOMeBn	11 ± 10	28 ± 12
18i	C(O)NHEt	3,4-diOMeBn	12 ± 1.4	-10 ± 9.6
18j	C(O)NHEt	3,4,5-triOMeBn	5 ± 6.9	-4 ± 1.2
19			28 ± 2.6	9 ± 9

[a] The percentage increase in arrested cells was calculated with reference to the vehicle control. The data represents the mean ± SEM observed in three independent experiments.

[b] Vincristine, as a positive control, was tested at a concentration of 100 nM. All other compounds were tested at 10 μM.

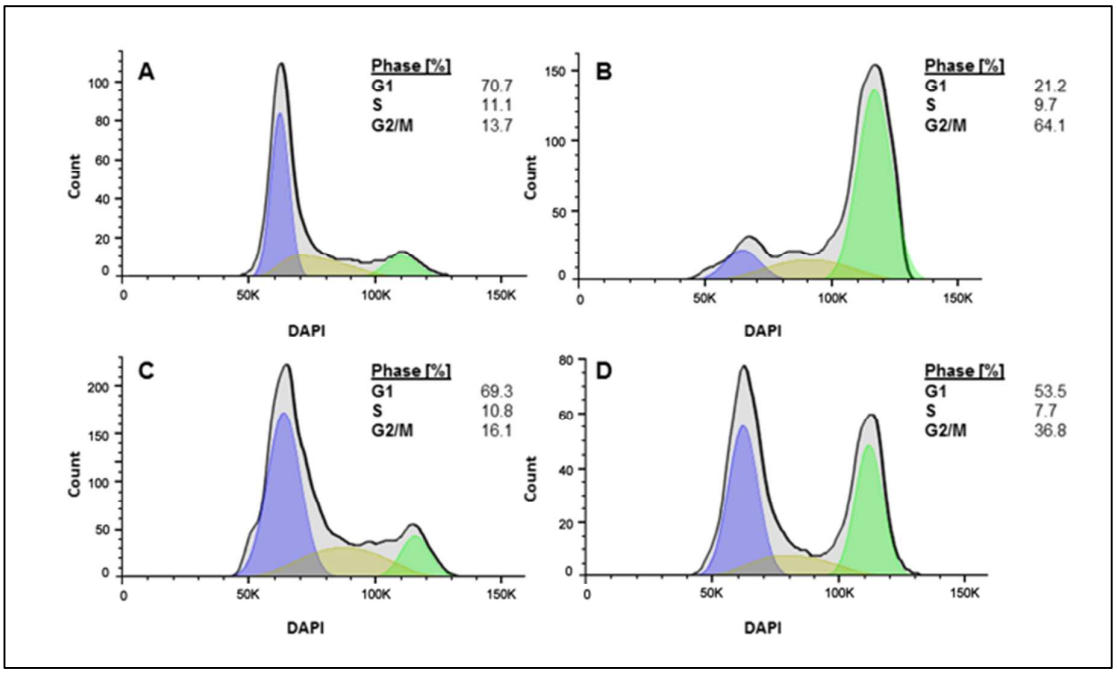

Figure 4. FACS analysis of PANC-1 cells treated for 18 h with (A) 0.1% DMSO, (B) vincristine (100 nM), (C) noscapine (**5**) (10 μM), (D) **18g** (10 μM). FACS data was processed with FlowJo (v10) and % cells were obtained at the G1 (blue), S (yellow) and G2/M (green) phases of the cell proliferation cycle.

Tubulin polymerisation assay. Cytotoxic agents that interfere with MT dynamics are often found to alter tubulin polymerisation through direct interaction with tubulin. For example, paclitaxel (**3**), a microtubule-stabilising agent, significantly enhances maximal initial velocity (V_{max}) in the growth phase of tubulin polymerisation, in comparison to control (tubulin with DMSO).[30] Conversely, the V_{max} of tubulin polymerisation was reduced in the presence of noscapine (**5**) (in a concentration-dependent manner).[5] This characteristic inhibition of microtubule assembly has also previously been observed with noscapinoids.[23] To ascertain that the anti-proliferative effect of **18g** against breast cancer cells are due to interactions with tubulin, **18g** was subjected to tubulin polymerisation experiments (**Fig. 5**). The control (DMSO + tubulin) represents normal rate of polymerisation in the absence of ligands (V_{max} = 27 ± 2 mOD/min). At 10 μM, paclitaxel (**3**) enhances polymerisation with a V_{max} of 76 ± 6 mOD/min. Noscapinoid **18g** was found to behave in a similar manner to parent noscapine (**5**), decreasing the initial polymerisation rate to 20 ± 2 mOD/min at 10 μM.

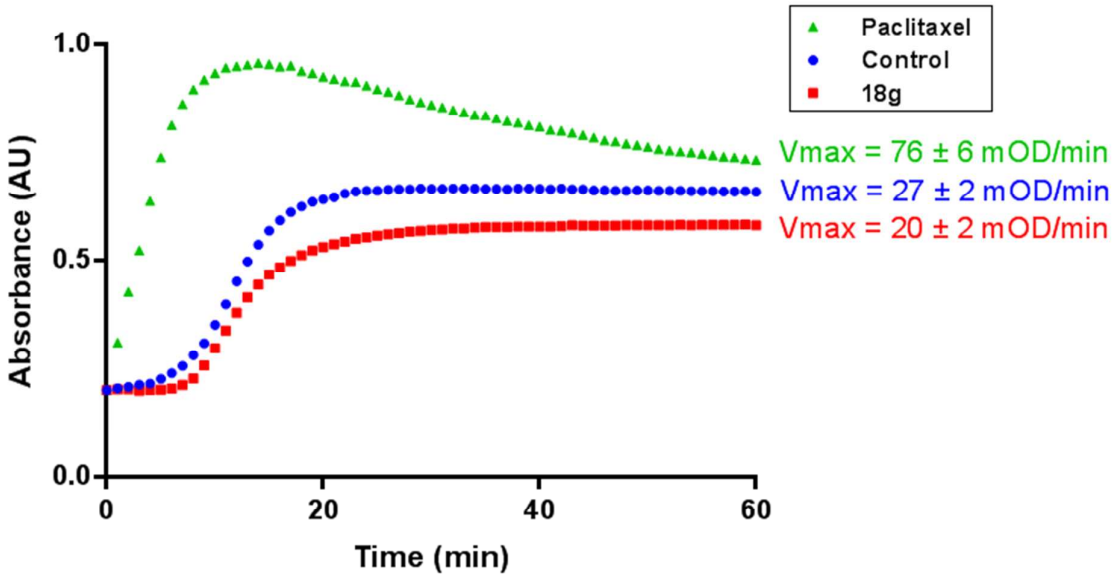

Figure 5. Tubulin polymerisation assay in the absence (in blue), and presence of ligand (paclitaxel, in green; **18g**, in red)

Compound 18g demonstrates efficacy in drug resistant cancer cells expressing P-gp. Noscapinoid **18g** demonstrates anti-proliferative activity by arrest of cells at the G2/M stage of the cell cycle. The mechanism of action involves tubulin perturbation; however, several tubulin disrupting drugs including paclitaxel and vinblastine are affected by the presence of P-gp. This efflux pump mediates their active extrusion from resistant cells and its influence on noscapine (**5**) and **18g** was investigated in a drug resistant variant (NCI/Adr^{RES}) of MCF-7^{WT} breast cancer cells.

The anti-proliferative efficacy was measured in both cell lines using a MTT assay and data shown in Table 2. The anticancer drug vinblastine caused potent inhibition of MCF-7^{WT} cell growth with an IC_{50} value of 0.36 ± 0.01 nM. The potency was reduced by ~267-fold in the drug resistant cells expressing high levels of P-gp. In contrast, the anti-proliferative effects of noscapine and **18g** did not differ between the two cell lines (Table 2). This demonstrates that the expression of P-gp does not alter the efficacy of these two compounds, in contrast to the TPI vinblastine.

Table 2. Cell proliferation, calcein transport and ATP hydrolysis profile of noscapine (5), 18g, nicardipine and vinblastine, in drug-sensitive (MCF-7^{WT}) and -resistant (NCI/Adr^{RES}) breast cancer cell lines.[a]

Drug	Cell Proliferation		Calcein-AM Transport	ATP Hydrolysis	
	Potency IC_{50}(μM)		Maximal rate *(RFU/min)*	Maximal rate *(fold-basal)*	Potency *IC_{50}(μM)*
	MCF-7	NCI/Adr^{RES}			
Noscapine (**5**)	18.8 ± 6.4	17.4 ± 4.5	26.7 ± 4.2	17.6 ± 2.8	69.7 ± 8.9
18g	2.7 ± 1.0	2.5 ± 1.3	78 ± 20	6.2 ± 1.1	2.4 ± 0.6
Nicardipine	--	--	107 ± 15	13.6 ± 2.3	4.7 ± 0.5
Vinblastine[b]	0.36 ± 0.01	96 ± 15	--	--	--

[a] Cells were treated with varying concentrations of test compounds and cell viability was determined using a standard MTT assay. Potency was determined by non-linear least squares regression of the sigmoidal dose-response equation. The data represented the mean ± SEM for at least 8 independent observations. [b] The IC_{50} values for vinblastine are in nM.

The above observation may offer the potential of synergy to generate growth arrest in cancer cells between noscapine derivatives and cytotoxic anticancer drugs. This would be of particular importance in resistant cells where P-gp generates an accumulation deficit. Therefore, the ability of noscapine (**5**) and **18g** to alter P-gp mediated transport was assessed using the fluorescent substrate calcein-AM. The calcein-AM rapidly accumulates in MCF-7 cells where it is cleaved to the highly fluorescent calcein, a charged species that is trapped in the cytoplasm.[31] Addition of **5**, **18g** or nicardipine failed to alter the rate of calcein accumulation in MCF-7^{WT} cells (data not shown). In contrast, the NCI/Adr^{RES} cells displayed negligible fluorescence over a 10 minute incubation period. The addition of the P-gp modulator nicardipine caused a rapid increase in fluorescent signal to a maximal rate of calcein accumulation in rate of 107 ± 15 RFU/min (Table 2). Noscapine (**5**) also elicited an increase in calcein accumulation, although the maximal rate was 4-fold lower than observed for nicardipine. Similarly, **18g** increased the fluorescent signal to 78 ± 20 RFU/min, which was 3-fold greater than the effect produced by noscapine (**5**). This data suggests that noscapine (**5**) and **18g** are able to modulate the transport activity of P-gp.

To ascertain whether the altered transport rate was due to direct interaction with P-gp, a more direct assay was used. P-gp was purified and reconstituted into lipid bilayers as previously described,[32,33] and drug dependent stimulation of ATP hydrolysis was measured. The basal rate of ATP hydrolysis by purified P-gp was 190 ± 40 nmol Pi/min/mg protein and this was stimulated to 1266 ± 197 nmol Pi/min/mg protein in the presence of 3 μM nicardipine. Full dose-response analysis of the effect of **5**, **18g** and nicardipine on ATP hydrolysis are summarised in Table 2. All three compounds produced significant stimulation of ATP hydrolysis by P-gp. The degree of stimulation by **18g** was less than that observed for noscapine (**5**), but its potency was significantly greater. This indicates that **18g** interacts directly with P-gp to modulate its function.

In summary, the anti-proliferative effects of noscapine and **18g** were unaffected by the presence of the resistance conferring efflux pump P-gp. Moreover, both compounds were able to directly modulate the function of P-gp. This offers the potential for co-administration of noscapine derivatives with anticancer drugs to achieve synergistic growth inhibitory effects, even in drug resistant cells. This activity could be potentially higher due to the fact this was not an enantioselective synthesis and presumably only one enantiomer would confer activity based on previous work.[26] Obviously, the activity of noscapine and 5-substituted THIQs is moderate and further work is continuing to increase the potency of these molecules.

Synergistic Effects. Both vinblastine and **18g** cause growth inhibitory effects by disruption of tubulin dynamics, although they bind to distinct sites on the tubulin monomer. Consequently, the two compounds may interact in a synergistic manner. To investigate this possibility, the effects of vinblastine on cell proliferation were measured in the presence of fixed concentrations of **18g** (Figure 6). In both cell lines the dose-response curves were shifted (by varying degrees) to the left, thus indicating a higher apparent potency (IC_{50}) for vinblastine in the presence of **18g**. The range of vinblastine concentrations used in the two cell lines differs and the shift in the curves was not equivalent. In addition, the upper level of the dose-response curve was reduced for increasing concentrations of **18g**, which reflects the inherent growth inhibitory effects of the noscapine derivatives.

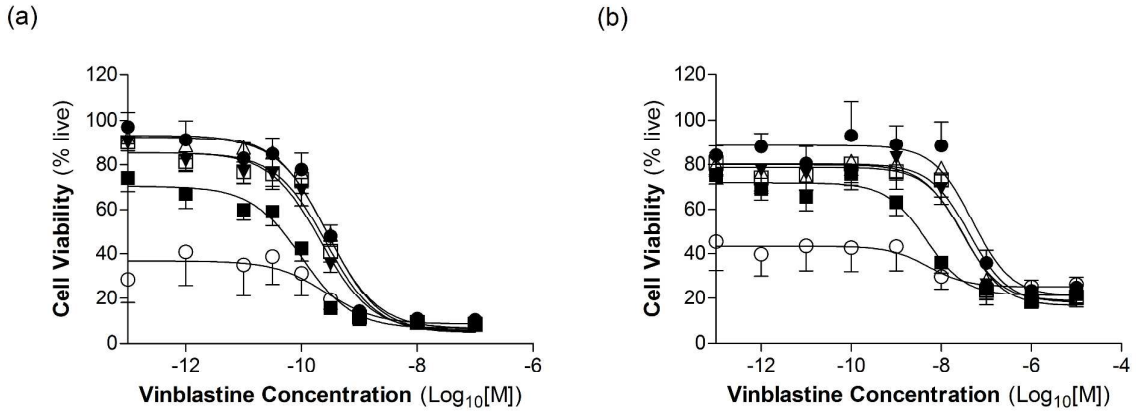

Figure 6. The effect of **18g** on the cytotoxicity of vinblastine in the drug-sensitive MCF-7^{WT} and the drug-resistant NCI/Adr^{RES} cells. The (a) MCF-7^{WT} and (b) NCI/Adr^{RES} cells were treated with varying concentrations of vinblastine alone (●) or in combination with 0.1 (Δ), 0.3 (□), 1.0 (▼), 3.0 (■) or 10 μM (○) of **18g** and incubated for 6 d. The cell viability was determined using a MTT assay and data fitted with the general dose-response relationship. All values represent mean ± SEM obtained from at least three independent observations.

Combination Index analysis provides a quantitative measure of the changes in dose-response curves and reveals whether the drug interactions are additive or synergistic.[34] Table 3 shows the combination indices (CI) for the combination of vinblastine and **18g** in both cell lines. In the MCF-7^{WT} cell line, the CI values did not differ significantly from 1.0 at any concentration of **18g**. This demonstrates an additive interaction between **18g** and vinblastine in MCF-7^{WT} cells. In contrast, the CI values obtained using **18g** concentrations of 0.3 and 0.1 μM were significantly different from 1.0 in the resistant cells. The values were <1.0 thereby demonstrating a synergistic interaction. The CI-value at a concentration of 1.0 μM of **18g** was not different to 1.0 and at higher concentrations of **18g**, the "downward shift" in the dose-response curve precluded accurate assignment of a CI-value. Thus, compound **18g** provides a novel route to restoration of the efficacy of chemotherapy in resistant cancer cells. It modulates the drug efflux activity of P-gp and the combined effects on tubulin result in a synergistic antiproliferative effect with vinblastine.

Table 3. Combination Indices for co-administration of 18g and vinblastine in MCF-7 and NCI/Adr^{RES} cells.

18g (μM)	MCF-7^{WT}	NCI/Adr^{RES}
1	1.50 ± 0.17	0.95 ± 0.18
0.3	1.02 ± 0.19	0.57 ± 0.11
0.1	1.09 ± 0.26	0.60 ± 0.17

Vinblastine and **18g** were co-administered to drug sensitive (MCF-7) and drug resistant (NCI/Adr^{RES}) cancer cells. Combination indices (CI) were calculated at 50% cell viability using Lowe's Additivity Model as described in the Experimental section. The CIs are represented as the mean ± SEM of at least 4 independent observations.

■ CONCLUSIONS

We have synthesised a series of 5-substituted THIQs **17a-j** and **18a-j** via a 10-step synthesis and two of these compounds (**17g** and **18g**) exhibited marked improvement in their ability to halt mitosis at the G2/M phase compared with noscapine (**5**). The 5-(4-methoxybenzyl) substituted analogue **18g** featuring a *N*-ethylcarbamoyl moiety produced a 208% increase in G2/M arrest in MCF-7 cells and a 175% increase in PANC-1 cells in a cell cycle arrest assay. Compound **18g** was assessed in a tubulin polymerisation assay and found to reduce the maximal initial velocity of tubulin polymerisation (V_{max}) relative to the control. This compound displayed an EC_{50} of 2.7 μM against a sensitive breast cancer line (MCF-7^{WT}), a 7-fold increase in potency relative to noscapine. This potency was maintained against a resistant breast cancer line (NCI/Adr^{RES}), which demonstrates the potential to limit resistance effects seen for most current cytotoxic agents. Furthermore, noscapine and **18g** were shown to interact directly with P-gp to modulate its function in an ATP hydrolysis assay. This highlights the potential for co-administration of noscapine and derivatives with anticancer drugs to achieve synergistic growth inhibitory effects.

■ EXPERIMENTAL SECTION

Chemistry. ^{1}H and ^{13}C NMR spectra were recorded on a Bruker Avance Nanobay III 400 MHz Ultrashield Plus spectrometer at 400.13 and 100.62 MHz, respectively coupled to a BACS 60 automatic sample changer at 25 °C. Chemical shifts (δ) are recorded in parts per million (ppm) by correction with reference to the chemical shift of the solvent, according to the procedure described by Gottlieb et al.[35] Coupling constants (*J*) are recorded in Hz, and the significant multiplicities described by singlet (s), doublet (d), triplet (t), quadruplet (q), broad (br), multiplet (m), doublet of doublets (dd), and doublet of triplets (dt). LC-MS were run to verify reaction outcome and purity using an Agilent 6100 series Single Quad coupled to an Agilent 1200 series HPLC. The following buffers were used: buffer A, 0.1% formic acid in H_2O; buffer B, 0.1% formic acid in MeCN. The following gradient was used with a Phenomenex Luna 3 μM C8(2) 15 mm × 4.6 mm column, and a flow rate of 0.5 mL/min and total run time of 12 min; 0–4 min 95% buffer A and 5% buffer B, 4–7 min 0% buffer A and 100% buffer B, 7–12 min 95% buffer A and 5% buffer B. Mass spectra were acquired in positive and negative ion mode with a scan range of 0–1000 *m*/*z* at 5 V. UV detection was carried out at 254 nm. All compounds were of >95% purity. Thin layer chromatography was conducted on 0.2 mm plates using Merck silica gel 60 F_{254}. Column chromatography was achieved using Merck silica gel 60 (particle size 0.063–0.200 μm, 70–230 mesh). Calculated partition co-efficient values (cLogP) were calculated using ChemAxon's Instant JChem program. Instant JChem was used for structure database management, search and prediction (Instant JChem 5.9.4, 2013, ChemAxon; http://www.chemaxon.com).]

General Procedure for the Formation of Amides 14a-j. To a stirred solution of 2-(4-bromo-7-methoxybenzo[*d*][1,3]dioxol-5-yl)ethan-1-amine (**13**) (typically 300 mg, 1.0 eq), HOBt (1.2 eq), EDCI.HCl (1.2 eq) and the appropriate phenylacetic or benzoic acid (1.01 eq) in DMF (3 mL) was added DIPEA (2.5 eq) and the solution stirred for 16 h at 25 °C. The solution was added dropwise to ice/water (~ 50 mL) and the resultant precipitate filtered, washed with water and dried thoroughly to give the corresponding amide **14**.

***N*-(2-(4-Bromo-7-methoxybenzo[*d*][1,3]dioxol-5-yl)ethyl)benzamide (14a).** Compound **14a** was formed in 92% as a colourless solid. ^{1}H NMR ($CDCl_3$) δ 7.76–7.71 (m, 2H), 7.52–7.47 (m, 1H), 7.40–7.45 (m, 2H), 6.47 (s, 1H), 6.20 (br s, 1H), 6.05 (s, 2H), 3.81 (s, 3H), 3.70 (t, *J* = 6.8 Hz, 2H), 3.02 (t, *J* = 6.9 Hz, 2H). ^{13}C NMR ($CDCl_3$) δ 167.7, 147.3, 143.0, 134.6, 134.4, 132.1, 131.7, 128.7 (× 2), 127.0 (× 2), 109.9, 102.0, 95.3, 56.8, 40.2, 34.8.

***N*-(2-(4-Bromo-7-methoxybenzo[*d*][1,3]dioxol-5-yl)ethyl)-4-methoxybenzamide (14b).** Compound **14b** was formed in 92% as a colourless solid. ^{1}H NMR ($CDCl_3$) δ 7.69 (d, *J* = 8.9 Hz, 2H), 6.91 (d, *J* = 8.9 Hz, 2H), 6.47 (s, 1H), 6.12 (br s, 1H), 6.04 (s, 2H), 3.84 (s, 3H), 3.81 (s, 3H), 3.67 (dd, *J* = 12.9, 6.8 Hz, 2H), 3.00 (t, *J* = 6.9 Hz, 2H). ^{13}C NMR ($CDCl_3$) δ 167.2, 162.4, 147.3, 143.0, 134.4, 132.2, 128.8 (× 2), 126.9, 113.9 (× 2), 109.9, 102.0, 95.4, 56.9, 55.6, 40.2, 34.9.

***N*-(2-(4-Bromo-7-methoxybenzo[*d*][1,3]dioxol-5-yl)ethyl)-2,3-dimethoxybenzamide (14c).** Compound **14c** was formed in 97% as a colourless solid. ^{1}H NMR ($CDCl_3$) δ 8.05 (t, *J* = 5.0 Hz, 1H), 7.71 (dd, *J* = 8.0, 1.6 Hz, 1H), 7.15 (t, *J* = 8.0 Hz, 1H), 7.03 (dd, *J* = 8.0, 1.6 Hz, 1H), 6.50 (s, 1H), 6.03 (s, 2H), 3.88 (s, 3H), 3.83 (s, 3H), 3.78 (s, 3H), 3.71 (dd, *J* = 13.0, 7.0 Hz, 2H), 3.01 (t, *J* = 7.0 Hz, 2H). ^{13}C NMR ($CDCl_3$) δ 165.4, 152.7, 147.6, 147.2, 142.9, 134.3, 132.2, 126.7, 124.5, 122.9, 115.5, 109.8, 101.9, 95.4, 61.3, 56.9, 56.2, 39.8, 34.9.

***N*-(2-(4-Bromo-7-methoxybenzo[*d*][1,3]dioxol-5-yl)ethyl)-4-methoxybenzamide (14d).** Compound **14d** was formed in 94% as a colourless solid. ^{1}H NMR ($CDCl_3$) δ 7.39 (d, *J* = 2.0 Hz, 1H), 7.21 (dd, *J* = 8.3, 2.0 Hz, 1H), 6.83 (d, *J* = 8.4 Hz, 1H), 6.45 (s, 1H), 6.24 (t, *J* = 5.6 Hz, 1H), 6.02 (s, 2H), 3.91 (s, 3H), 3.90 (s, 3H), 3.80 (s, 3H), 3.66 (dd, *J* = 12.9, 6.8 Hz, 2H), 3.00 (t, *J* = 6.9 Hz, 2H). ^{13}C NMR ($CDCl_3$) δ 167.3, 151.8, 149.1, 147.2, 143.0, 134.4, 132.2, 127.2, 119.3, 110.6, 1110.4, 109.9, 102.0, 95.3, 56.8, 56.1, 40.3, 34.8.

***N*-(2-(4-Bromo-7-methoxybenzo[*d*][1,3]dioxol-5-yl)ethyl)-3,4,5-trimethoxybenzamide (14e).** Compound **14b** was formed in 98% as a colourless solid. ^{1}H NMR ($CDCl_3$) δ 6.95 (s, 2H), 6.48 (s, 1H), 6.12 (t, *J* = 5.4 Hz, 1H), 6.04 (s, 2H), 3.89 (s, 6H), 3.88 (s, 3H), 3.84 (s, 3H), 3.68 (dd, *J* = 12.8, 6.8 Hz, 2H), 3.02 (t, *J* = 6.9 Hz, 2H). ^{13}C NMR ($CDCl_3$) δ 167.5, 153.4 (× 2), 147.3, 143.1, 141.1, 134.5, 132.2, 130.1, 110.2, 104.4, 102.0 (× 2), 95.5, 61.1, 57.0, 56.5 (× 2), 40.5, 34.7.

***N*-(2-(4-Bromo-7-methoxybenzo[*d*][1,3]dioxol-5-yl)ethyl)-2-phenylacetamide (14f).** Compound **14f** was formed in 93% as a colourless solid. ^{1}H NMR ($CDCl_3$) δ 7.36–7.27 (m, 3H), 7.24–7.18 (m, 2H), 6.33 (s, 1H), 6.02 (s, 2H), 5.45 (br s, 1H), 3.83 (s, 3H), 3.56 (s, 2H), 3.45 (dd, *J* = 13.1, 6.8 Hz, 2H), 2.82 (t, *J* = 6.9 Hz, 2H). ^{13}C NMR ($CDCl_3$) δ 171.2, 147.2, 142.9, 134.8, 134.3, 131.9, 129.6 (× 2), 129.1 (× 2), 127.5, 109.9, 101.9, 95.3, 57.0, 44.0, 39.7, 34.7.

***N*-(2-(4-Bromo-7-methoxybenzo[*d*][1,3]dioxol-5-yl)ethyl)-2-(4-methoxyphenyl)acetamide (14g).** Compound **14g** was formed in 94% as a colourless solid. ^{1}H NMR ($CDCl_3$) δ 7.13–7.09 (m, 2H), 6.88–6.83 (m, 2H), 6.32 (s, 1H), 6.03 (s, 2H), 5.39 (br s, 1H), 3.84 (s, 3H), 3.81 (s, 3H), 3.49 (s, 2H), 3.44 (dd, *J* = 12.9, 6.8 Hz, 2H), 2.81 (t, *J* = 6.8 Hz, 2H). ^{13}C NMR ($CDCl_3$) δ 171.6, 159.0, 147.2, 142.9, 134.4, 131.9, 130.7 (× 2), 126.7, 114.6 (× 2), 109.9, 101.9, 95.3, 57.0, 55.4, 43.1, 39.7, 34.7.

***N*-(2-(4-Bromo-7-methoxybenzo[*d*][1,3]dioxol-5-yl)ethyl)-2-(2,3-dimethoxyphenyl)acetamide (14h).** Compound **14h** was formed in 93% as a colourless solid. ^{1}H NMR ($CDCl_3$) δ 7.04–6.98 (m, 1H), 6.88–6.80 (m, 2H), 6.36 (s, 1H), 6.01 (s, 2H), 5.92 (br s, 1H), 3.87 (s, 3H), 3.84 (s, 3H), 3.81 (s, 3H), 3.54 (s, 2H), 3.41 (dd, *J* = 13.1, 6.9 Hz, 2H), 2.81 (t, *J* = 7.0 Hz, 2H). ^{13}C NMR ($CDCl_3$) δ 171.3, 153.0, 147.1, 147.0, 142.9, 134.3, 132.1, 129.2, 124.6, 122.9, 111.9, 109.8, 101.9, 95.4, 60.7, 56.9, 55.8, 39.7, 38.8, 34.9.

***N*-(2-(4-Bromo-7-methoxybenzo[*d*][1,3]dioxol-5-yl)ethyl)-2-(3,4-dimethoxyphenyl)acetamide (14i).** Compound **14i** was formed in 94% as a colourless solid. ^{1}H NMR ($CDCl_3$) δ 6.81 (d, *J* = 8.0 Hz, 1H), 6.74–6.69 (m, 2H), 6.33 (s, 1H), 6.03 (s, 2H), 5.43 (t, *J* = 4.7 Hz, 1H), 3.88 (s, 3H), 3.85 (s, 3H), 3.84 (s, 3H), 3.49 (s, 2H), 3.45 (dd, *J* = 12.9, 6.9 Hz, 2H), 2.82 (t, *J* = 6.9 Hz, 2H). ^{13}C NMR ($CDCl_3$) δ 171.5, 149.4, 148.5, 147.2, 142.9, 134.3, 131.8, 127.2, 121.7, 112.5, 111.6, 109.8, 101.9, 95.3, 56.9, 56.0, 55.9, 43.6, 39.8, 34.5.

***N*-(2-(4-Bromo-7-methoxybenzo[*d*][1,3]dioxol-5-yl)ethyl)-2-(3,4,5-trimethoxyphenyl)acetamide (14j).** Compound **14j** was formed in 87% as a colourless solid. ^{1}H NMR ($CDCl_3$) δ 6.41 (s, 2H), 6.36 (s, 1H), 6.03 (s, 2H), 5.51 (t, *J* = 5.5 Hz, 1H), 3.85 (s, 3H), 3.84 (s, 3H), 3.83 (s, 6H), 3.50–3.43 (m, 4H), 2.85 (t, *J* = 6.9 Hz, 2H). ^{13}C NMR ($CDCl_3$) δ 171.1, 153.7

(× 2), 147.2, 142.9, 137.3, 134.3, 131.9, 130.3, 109.8, 106.5 (× 2), 101.9, 95.4, 61.0, 57.0, 56.2 (× 2), 44.3, 40.0, 34.4.

General Procedure for the Bischler-Napieralski cyclisation (compounds 15a-j). To a mixture of the amide **14** (typically 300 mg, 1.0 eq) in toluene (3 mL) in a teflon-capped sealed tube was added $POCl_3$ (5.0 eq) dropwise. The fluffy white mixture was heated at 120 °C for 2 h. The yellow solution, which formed, was cooled to room temperature and added to DCM (30 mL). Saturated $NaHCO_3$ (20 mL) and 5 M KOH (0.5 mL) were carefully added and stirred for 30 min. The organic phase was separated, washed with sat. $NaHCO_3$ (20 mL) and 5 M KOH (0.5 mL), then sat. NaCl, dried with $MgSO_4$, filtered and the filtrate evaporated under reduced pressure to give the cyclised imine **15**. This was immediately taken forward in the reduction step.

9-Bromo-4-methoxy-5-phenyl-7,8-dihydro-[1,3]dioxolo[4,5-*g*]isoquinoline (15a). Compound **15a** was formed in 95% as a yellow gum. ^{1}H NMR ($CDCl_3$) δ 7.47–7.42 (m, 2H), 7.40–7.37 (m, 3H), 6.06 (s, 2H), 3.74–3.66 (m, 2H), 3.49 (s, 3H), 2.79–2.72 (m, 2H).

9-Bromo-4-methoxy-5-(4-methoxyphenyl)-7,8-dihydro-[1,3]dioxolo[4,5-*g*]isoquinoline (15b). Compound **15b** was formed in 94% as a yellow gum. ^{1}H NMR ($CDCl_3$) δ 7.45 (d, J = 8.8 Hz, 2H), 6.90 (d, J = 8.9 Hz, 2H), 6.07 (s, 2H), 3.83 (s, 3H), 3.72 – 3.64 (m, 2H), 3.57 (s, 3H), 2.82–2.72 (m, 2H).

9-Bromo-5-(2,3-dimethoxyphenyl)-4-methoxy-7,8-dihydro-[1,3]dioxolo[4,5-*g*]isoquinoline (15c). Compound **15c** was formed in 86% as a yellow gum. ^{1}H NMR ($CDCl_3$) δ 7.08 (t, J = 7.9 Hz, 1H), 6.96 (dd, J = 7.7, 1.6 Hz, 1H), 6.90 (dd, J = 8.1, 1.5 Hz, 1H), 6.00 (s, 2H), 4.05–3.95 (m, 1H), 3.86 (s, 3H), 3.57 (s, 3H), 3.44 (s, 3H), 2.94–2.82 (m, 2H), 2.67–2.55 (m, 1H).

9-Bromo-5-(3,4-dimethoxyphenyl)-4-methoxy-7,8-dihydro-[1,3]dioxolo[4,5-*g*]isoquinoline (15d). Compound **15d** was formed in 99% as a yellow oil. ^{1}H NMR ($CDCl_3$) δ 7.37 (d, J = 1.5 Hz, 1H), 7.16 (d, J = 6.7 Hz, 1H), 6.93 (d, J = 8.5 Hz, 1H), 6.19 (s, 2H), 4.02 (s, 3H), 3.94 (s, 3H), 3.90 – 3.83 (m, 2H), 3.70 (s, 3H), 3.09–3.01 (m, 2H).

9-Bromo-4-methoxy-5-(3,4,5-trimethoxyphenyl)-7,8-dihydro-[1,3]dioxolo[4,5-*g*]isoquinoline (15e). Compound **15e** was formed in 98% as a yellow gum. ^{1}H NMR ($CDCl_3$) δ

6.75 (s, 2H), 6.10 (s, 2H), 3.88 (s, 6H), 3.87 (s, 3H), 3.75–3.69 (m, 2H), 3.60 (s, 3H), 2.84–2.78 (m, 2H).

5-Benzyl-9-bromo-4-methoxy-7,8-dihydro-[1,3]dioxolo[4,5-*g*]isoquinoline (15f). Compound **15f** was formed in 98% as an orange gum. ^{1}H NMR ($CDCl_3$) δ 7.32–7.25 (m, 2H), 7.24–7.19 (m, 3H), 6.05 (s, 2H), 4.41 (s, 2H), 3.93 (s, 3H), 3.68 – 3.62 (m, 2H), 2.80–2.72 (m, 2H).

9-Bromo-4-methoxy-5-(4-methoxybenzyl)-7,8-dihydro-[1,3]dioxolo[4,5-*g*]isoquinoline (15g). Compound **15g** was formed in 95% as an orange gum. ^{1}H NMR ($CDCl_3$) δ 7.08 (d, J = 8.7 Hz, 2H), 6.77 (d, J = 8.7 Hz, 2H), 6.00 (s, 2H), 4.20 (br s, 2H), 3.90 (s, 3H), 3.75 (s, 3H), 3.58–3.52 (m, 2H), 2.68–2.61 (m, 2H).

9-Bromo-5-(2,3-dimethoxybenzyl)-4-methoxy-7,8-dihydro-[1,3]dioxolo[4,5-*g*]isoquinoline (15h). Compound **15h** was formed in 99% as a yellow gum. ^{1}H NMR ($CDCl_3$) δ 6.91 (t, J = 7.9 Hz, 1H), 6.76 (dd, J = 8.2, 1.4 Hz, 1H), 6.66–6.57 (m, 1H), 5.98 (s, 2H), 4.21 (s, 2H), 3.84 (s, 3H), 3.82 (s, 3H), 3.78 (s, 3H), 3.53 (dd, J = 7.7, 6.6 Hz, 2H), 2.64 (dd, J = 7.9, 6.5 Hz, 2H).

9-Bromo-5-(3,4-dimethoxybenzyl)-4-methoxy-7,8-dihydro-[1,3]dioxolo[4,5-*g*]isoquinoline (15i). Compound **15i** was formed in 96% as a yellow gum. ^{1}H NMR ($CDCl_3$) δ 6.74–6.68 (m, 3H), 5.99 (s, 2H), 4.15 (s, 2H), 3.90 (s, 3H), 3.82 (s, 3H), 3.80 (s, 3H), 3.56–3.49 (m, 2H), 2.63–2.58 (m, 2H).

9-Bromo-4-methoxy-5-(3,4,5-trimethoxybenzyl)-7,8-dihydro-[1,3]dioxolo[4,5-*g*]isoquinoline (15j). Compound **15j** was formed in 94% as a yellow gum. ^{1}H NMR ($CDCl_3$) δ 6.40 (s, 2H), 6.00 (s, 2H), 4.14 (s, 2H), 3.92 (s, 3H), 3.79 (s, 3H), 3.78 (s, 6H), 3.56–3.51 (m, 2H), 2.64–2.59 (m, 2H).

General Procedure for Imine Reduction (compounds 16a-j). The imine **15** (typically 275 mg, 1.0 eq) was taken up in MeOH (3 mL), cooled to -78 °C and $NaBH_4$ (3.0 eq) added portionwise. The reaction was stirred at this temperature for 30 min, then allowed to slowly warm up to room temperature. Water (5 mL) and sat. NaCl (10 mL) were added and extracted with DCM (2 × 25 mL), dried with $MgSO_4$, filtered and the filtrate evaporated under reduced pressure to give the reduced tetrahydroisoquinoline **16**.

9-Bromo-4-methoxy-5-phenyl-5,6,7,8-tetrahydro-[1,3]dioxolo[4,5-*g*]isoquinoline (16a). Compound **16a** was formed in 94% as a yellow solid. ^{1}H NMR ($CDCl_3$) δ 7.31–7.20 (m, 3H), 7.15–7.11 (m, 2H), 5.99 (d, *J* = 1.4 Hz, 1H), 5.97 (d, *J* = 1.4 Hz, 1H), 5.25 (s, 1H), 3.52 (s, 3H), 2.99–2.87 (m, 2H), 2.77–2.65 (m, 2H).

9-Bromo-4-methoxy-5-(4-methoxyphenyl)-5,6,7,8-tetrahydro-[1,3]dioxolo[4,5-*g*]isoquinoline (16b). Compound **16b** was formed in 85% as a mauve solid. ^{1}H NMR ($CDCl_3$) δ 6.98 (d, *J* = 8.6 Hz, 2H), 6.75 (d, *J* = 8.6 Hz, 2H), 5.91 (d, *J* = 1.2 Hz, 1H), 5.90 (d, *J* = 1.2 Hz, 1H), 5.16 (s, 1H), 3.71 (s, 3H), 3.48 (s, 3H), 2.91–2.79 (m, 2H), 2.71–2.56 (m, 2H).

9-Bromo-5-(2,3-dimethoxyphenyl)-4-methoxy-5,6,7,8-tetrahydro-[1,3]dioxolo[4,5-*g*]isoquinoline (16c). Compound **16c** was formed in 90% as a yellow solid. ^{1}H NMR ($CDCl_3$) δ 6.90 – 6.81 (m, 2H), 6.26 (dd, *J* = 7.4, 1.7 Hz, 1H), 5.98 (dd, *J* = 4.0, 1.4 Hz, 2H), 5.60 (s, 1H), 3.95 (s, 3H), 3.89 (s, 3H), 3.60 (s, 3H), 2.93–2.79 (m, 2H), 2.74–2.70 (m, 2H).

9-Bromo-5-(3,4-dimethoxyphenyl)-4-methoxy-5,6,7,8-tetrahydro-[1,3]dioxolo[4,5-*g*]isoquinoline (16d). Compound **16d** was formed in 47% as a mauve solid. ^{1}H NMR ($CDCl_3$) δ 6.86 (d, *J* = 1.7 Hz, 1H), 6.74 (d, *J* = 8.3 Hz, 1H), 6.51 (dd, *J* = 8.2, 1.9 Hz, 1H), 5.99 (s, 2H), 5.27 (s, 1H), 3.88 (s, 3H), 3.85 (s, 3H), 3.58 (s, 3H), 3.03 – 2.90 (m, 2H), 2.79–2.69 (m, 2H).

9-Bromo-4-methoxy-5-(3,4,5-trimethoxyphenyl)-5,6,7,8-tetrahydro-[1,3]dioxolo[4,5-*g*]isoquinoline (16e). Compound **16e** was formed in 80% as a yellow solid. ^{1}H NMR ($CDCl_3$) δ 6.38 (s, 2H), 6.01 (d, *J* = 1.3 Hz, 1H), 6.00 (d, *J* = 1.3 Hz, 1H), 5.25 (s, 1H), 3.83 (s, 3H), 3.81 (s, 6H), 3.61 (s, 3H), 3.03 – 2.94 (m, 2H), 2.83 – 2.69 (m, 2H).

5-Benzyl-9-bromo-4-methoxy-5,6,7,8-tetrahydro-[1,3]dioxolo[4,5-*g*]isoquinoline (16f). Compound **16f** was formed in 92% as a yellow solid. ^{1}H NMR ($CDCl_3$) δ 7.38–7.31 (m, 2H), 7.30–7.21 (m, 3H), 6.00 (d, *J* = 1.4 Hz, 1H), 5.97 (d, J = 1.4 Hz, 1H), 4.25 (dd, *J* = 10.5, 2.8 Hz, 1H), 4.07 (s, 3H), 3.24 (ddd, *J* = 12.3, 10.8, 5.2 Hz, 1H), 3.03 (ddd, *J* = 12.4, 5.5, 2.7 Hz, 2H), 2.84 (dd, *J* = 13.7, 10.5 Hz, 1H), 2.77–2.59 (m, 2H).

9-Bromo-4-methoxy-5-(4-methoxybenzyl)-5,6,7,8-tetrahydro-[1,3]dioxolo[4,5-*g*]isoquinoline (16g). Compound **16g** was formed in 71% as a yellow solid. ^{1}H NMR ($CDCl_3$) δ

7.19 (d, *J* = 8.5 Hz, 2H), 6.89 (d, *J* = 8.6 Hz, 2H), 5.98 (dd, *J* = 8.7, 1.4 Hz, 2H), 4.19 (dd, *J* = 10.5, 2.8 Hz, 1H), 4.07 (s, 3H), 3.81 (s, 3H), 3.28–3.17 (m, 1H), 3.06–2.92 (m, 2H), 2.82–2.58 (m, 3H).

9-Bromo-5-(2,3-dimethoxybenzyl)-4-methoxy-5,6,7,8-tetrahydro-[1,3]dioxolo[4,5-*g*]isoquinoline (16h). Compound **16h** was formed in 54% as a colourless solid. ^{1}H NMR ($CDCl_3$) δ 7.04 (t, *J* = 7.9 Hz, 1H), 6.87 (dd, *J* = 7.7, 1.4 Hz, 1H), 6.82 (dd, *J* = 8.1, 1.3 Hz, 1H), 5.98 (d, *J* = 1.3 Hz, 1H), 5.96 (d, *J* = 1.3 Hz, 1H), 4.32 (t, *J* = 6.8 Hz, 1H), 4.05 (s, 3H), 3.88 (s, 3H), 3.85 (s, 3H), 3.33–3.23 (m, 1H), 3.04–2.94 (m, 3H), 2.75–2.55 (m, 2H).

9-Bromo-5-(3,4-dimethoxybenzyl)-4-methoxy-5,6,7,8-tetrahydro-[1,3]dioxolo[4,5-*g*]isoquinoline (16i). Compound **16i** was formed in 81% as a yellow solid. ^{1}H NMR ($CDCl_3$) δ 6.87 – 6.77 (m, 3H), 5.99 (dd, *J* = 9.1, 1.4 Hz, 2H), 4.23 (dd, *J* = 10.3, 2.8 Hz, 1H), 4.07 (s, 3H), 3.90 (s, 3H), 3.88 (s, 3H), 3.21 (ddd, *J* = 12.3, 10.3, 5.4 Hz, 1H), 3.05–2.94 (m, 2H), 2.78 (dd, *J* = 13.8, 10.4 Hz, 1H), 2.73–2.58 (m, 2H).

9-Bromo-4-methoxy-5-(3,4,5-trimethoxybenzyl)-5,6,7,8-tetrahydro-[1,3]dioxolo[4,5-*g*]isoquinoline (16j). Compound **16j** was formed in 78% as a yellow solid. ^{1}H NMR ($CDCl_3$) δ 6.48 (s, 2H), 5.99 (dd, *J* = 9.6, 1.4 Hz, 2H), 4.27 (dd, *J* = 10.3, 2.8 Hz, 1H), 4.07 (s, 3H), 3.88 (s, 6H), 3.85 (s, 3H), 3.21 (ddd, *J* = 12.4, 10.3, 5.4 Hz, 1H), 3.07–2.94 (m, 2H), 2.81–2.59 (m, 3H).

General Procedure for N-Methylation (compounds 17a-j). Method A. To a stirred mixture of THIQ (**16**) (typically 100 mg, 1.0 eq) and K_2CO_3 (2.5 eq) in DMF (1 mL) cooled on ice, was added MeI (1.1 eq) dropwise and the reaction stirred at 25 °C for 3 h. Water (15 mL) was added and extracted with EtOAc (30 mL). The aqueous fraction was re-extracted with EtOAc (10 mL). The combined organic fractions were washed with water (3 × 10 mL), sat. NaCl, dried with $MgSO_4$, filtered and the filtrate evaporated under reduced pressure to give the reduced N-methyl product **17**.

Method B.[36] To a stirred solution of THIQ (**16**) (typically 100 mg, 1.0 eq) in HCOOH (1 mL) was added CH_2O solution (37% wt. in water) (7.0 eq) dropwise. The reaction was heated at 80 °C for 2 h and the resultant brown solution was cooled to room temperature. The mixture was then basified with 5 M NaOH to pH 9, extracted with EtOAc (3 × 15 mL), dried with $MgSO_4$, filtered and the filtrate evaporated under reduced pressure to give the reduced N-methyl product **17**.

9-Bromo-4-methoxy-6-methyl-5-phenyl-5,6,7,8-tetrahydro-[1,3]dioxolo[4,5-*g*]isoquinoline (17a). Compound **17a** was formed via Method A in 14% as a colourless oil. ^{1}H NMR ($CDCl_3$) δ 7.31–7.19 (m, 3H), 7.12–7.07 (m, 2H), 5.96 (dd, *J* = 9.7, 1.3 Hz, 2H), 4.77 (s, 1H), 3.38 (s, 3H), 2.93–2.73 (m, 3H), 2.67–2.61 (m, 1H), 2.35 (s, 3H). ^{13}C NMR ($CDCl_3$) δ 146.2, 141.6, 139.9, 135.5, 129.5 (× 2), 127.9, 127.7 (× 2), 127.0, 125.2, 101.2, 96.4, 63.6, 59.0, 46.2, 42.6, 27.6. HR-ESMS calcd. for $C_{18}H_{19}BrNO_3^+$ [M + H] 376.0543, found 376.0548.

9-Bromo-4-methoxy-5-(4-methoxyphenyl)-6-methyl-5,6,7,8-tetrahydro-[1,3]dioxolo[4,5-*g*]isoquinoline (17b). Compound **17b** was formed via Method B in 83% as a yellow oil. ^{1}H NMR ($CDCl_3$) δ 7.03–6.97 (m, 2H), 6.82–6.74 (m, 2H), 5.95 (d, *J* = 1.2 Hz, 1H), 5.93 (d, *J* = 1.3 Hz, 1H), 4.77 (s, 1H), 3.76 (s, 3H), 3.43 (s, 3H), 2.90–2.71 (m, 3H), 2.62 (dt, *J* = 9.0, 3.5 Hz, 1H), 2.33 (s, 3H). ^{13}C NMR ($CDCl_3$) δ 158.6, 146.1, 139.8, 135.4, 133.3, 130.5 (× 2), 127.6, 125.3, 113.0 (× 2), 101.1, 96.3, 62.6, 59.1, 55.3, 45.8, 42.4, 27.5. HR-ESMS calcd. for $C_{19}H_{21}BrNO_4^+$ [M + H] 406.0648, found 406.0640.

9-Bromo-5-(2,3-dimethoxyphenyl)-4-methoxy-6-methyl-5,6,7,8-tetrahydro-[1,3]dioxolo[4,5-*g*]isoquinoline (17c). Compound **17c** was formed via Method A in 26% as a colourless solid. ^{1}H NMR ($CDCl_3$) δ 6.88 (t, *J* = 7.9 Hz, 1H), 6.80 (dd, *J* = 8.2, 1.5 Hz, 1H), 6.31 (dd, *J* = 7.7, 1.6 Hz, 1H), 5.94 (dd, *J* = 10.0, 1.4 Hz, 2H), 5.31 (s, 1H), 3.94 (s, 3H), 3.88 (s, 3H), 3.46 (s, 3H), 2.93–2.72 (m, 3H), 2.65–2.56 (m, 1H), 2.35 (s, 3H). ^{13}C NMR ($CDCl_3$) δ 152.6, 147.7, 146.1, 139.6, 135.3, 134.9, 128.2, 125.6, 122.9, 122.0, 111.2, 101.1, 96.3, 60.3, 58.8, 55.9 (× 2), 46.1, 42.2, 27.8. HR-ESMS calcd. for $C_{20}H_{23}BrNO_5^+$ [M + H] 436.0754, found 436.0765.

9-Bromo-5-(3,4-dimethoxyphenyl)-4-methoxy-6-methyl-5,6,7,8-tetrahydro-[1,3]dioxolo[4,5-*g*]isoquinoline (17d). Compound **17d** was formed via Method B in 83% as a colourless oil. ^{1}H NMR ($CDCl_3$) δ 6.79–6.68 (m, 2H), 6.51 (dd, *J* = 8.2, 1.9 Hz, 1H), 5.95 (d, *J* = 0.9 Hz, 1H), 5.94 (d, *J* = 1.0 Hz, 1H), 4.75 (s, 1H), 3.84 (s, 3H), 3.83 (s, 3H), 3.45 (s, 3H), 2.93–2.56 (m, 4H), 2.35 (s, 3H). ^{13}C NMR ($CDCl_3$) δ 148.4, 148.1, 146.2, 139.9, 135.4, 134.1, 127.6, 125.0, 121.7, 113.1, 110.2, 101.2, 96.3, 63.0, 59.2, 56.1, 55.9, 45.7, 42.5, 27.1. HR-ESMS calcd. for $C_{20}H_{23}BrNO_5^+$ [M + H] 436.0754, found 436.0758.

9-Bromo-4-methoxy-6-methyl-5-(3,4,5-trimethoxyphenyl)-5,6,7,8-tetrahydro-[1,3]dioxolo[4,5-*g*]isoquinoline (17e). Compound **17e** was formed via Method B in 85% as a yellow oil. ^{1}H NMR ($CDCl_3$) δ 6.32 (s, 2H), 5.97 (d, *J* = 1.3 Hz, 1H), 5.97 (d, *J* = 1.3 Hz, 1H), 4.72 (s, 1H), 3.81 (s, 3H), 3.79 (s, 6H), 3.49 (s, 3H), 2.99–2.90 (m, 1H), 2.89–2.79 (m, 1H), 2.77–2.62 (m, 2H), 2.38 (s, 3H). ^{13}C NMR ($CDCl_3$) δ 152.6 (× 2), 146.3, 140.0, 137.5, 137.2, 135.4, 127.7, 124.6, 106.9 (× 2), 101.2, 96.3, 63.7, 60.9, 59.1, 56.4 (× 2), 46.1, 42.6, 27.0. HR-ESMS calcd. for $C_{21}H_{25}BrNO_6^+$ [M + H] 466.0860, found 466.0869.

5-Benzyl-9-bromo-4-methoxy-6-methyl-5,6,7,8-tetrahydro-[1,3]dioxolo[4,5-*g*]isoquinoline (17f). Compound **17f** was formed via Method A in 18% as a colourless oil. ^{1}H NMR ($CDCl_3$) δ 7.32–7.25 (m, 4H), 7.22–7.17 (m, 1H), 5.97 (dd, *J* = 5.5, 1.4 Hz, 2H), 4.01 (dd, *J* = 7.9, 4.7 Hz, 1H), 3.98 (s, 3H), 3.32 (ddd, *J* = 13.6, 11.3, 5.5 Hz, 1H), 2.91–2.78 (m, 3H), 2.70 (ddd, *J* = 17.7, 11.3, 6.8 Hz, 1H), 2.45 (ddd, *J* = 17.5, 5.5, 1.7 Hz, 1H), 2.29 (s, 3H). ^{13}C NMR ($CDCl_3$) δ 146.8, 141.3, 140.0, 134.4, 129.2 (× 2), 128.2 (× 2), 127.1, 125.9, 125.2, 100.9, 96.2, 60.3, 59.3, 44.0, 42.3, 40.7, 23.2. HR-ESMS calcd. for $C_{19}H_{21}BrNO_3^+$ [M + H] 390.0699, found 390.0707.

9-Bromo-4-methoxy-5-(4-methoxybenzyl)-6-methyl-5,6,7,8-tetrahydro-[1,3]dioxolo[4,5-*g*]isoquinoline (17g). Compound **17g** was formed via Method A in 36% as a colourless oil. ^{1}H NMR ($CDCl_3$) δ 7.17 (d, *J* = 8.6 Hz, 2H), 6.83 (d, *J* = 8.7 Hz, 2H), 5.97 (d, *J* = 1.4 Hz, 1H), 5.96 (d, *J* = 1.4 Hz, 1H), 3.97 (s, 3H), 3.79 (s, 3H), 3.36–3.25 (m, 1H), 2.87 (dd, *J* = 13.6, 6.2 Hz, 1H), 2.79 (d, *J* = 6.1 Hz, 2H), 2.76–2.64 (m, 2H), 2.45 (ddd, *J* = 7.1, 5.3, 1.3 Hz, 1H), 2.31 (s, 3H). ^{13}C NMR ($CDCl_3$) δ 157.9, 145.9, 140.0, 134.4, 133.0, 130.1 (× 2), 126.9, 113.7 (× 2), 101.2, 100.9, 96.1, 60.5, 59.4, 55.3, 44.0, 42.2, 39.7, 23.2. HR-ESMS calcd. for $C_{20}H_{23}BrNO_4^+$ [M + H] 420.0805, found 420.0810.

9-Bromo-5-(2,3-dimethoxybenzyl)-4-methoxy-6-methyl-5,6,7,8-tetrahydro-[1,3]dioxolo[4,5-*g*]isoquinoline (17h). Compound **17h** was formed via Method A in 12% as a yellow oil. ^{1}H NMR ($CDCl_3$) δ 7.00 (t, *J* = 7.9 Hz, 1H), 6.88 (dd, *J* = 7.7, 1.4 Hz, 1H), 6.78 (dd, *J* = 8.1, 1.4 Hz, 1H), 5.97 (d, *J* = 1.4 Hz, 1H), 5.95 (d, *J* = 1.4 Hz, 1H), 4.14 (dd, *J* = 9.8, 4.0 Hz, 1H), 3.94 (s, 3H), 3.86 (s, 3H), 3.84 (s, 3H), 3.38 (ddd, *J* = 13.6, 11.5, 5.8 Hz, 1H), 2.97 (dd, *J* = 14.1, 9.8 Hz, 1H), 2.89–2.78

(m, 2H), 2.70 (ddd, *J* = 18.2, 11.4, 7.1 Hz, 1H), 2.49 (ddd, *J* = 17.5, 5.6, 1.3 Hz, 1H), 2.28 (s, 3H). ^{13}C NMR ($CDCl_3$) δ 152.8, 147.6, 145.7, 140.2, 134.8, 134.5, 127.1, 125.6, 123.7, 122.5, 110.2, 100.8, 96.3, 60.7, 59.4, 59.2, 55.8, 43.6, 42.1, 33.9, 23.2. HR-ESMS calcd. for $C_{21}H_{25}BrNO_5^+$ [M + H] 450.0911, found 450.0928.

9-Bromo-5-(3,4-dimethoxybenzyl)-4-methoxy-6-methyl-5,6,7,8-tetrahydro-[1,3]dioxolo[4,5-*g*]isoquinoline (17i). Compound **17i** was formed via Method A in 37% as a pale yellow oil. ^{1}H NMR ($CDCl_3$) δ 6.82–6.78 (m, 3H), 5.96 (dd, *J* = 7.3, 1.4 Hz, 2H), 4.00–3.94 (m, 4H), 3.87 (s, 3H), 3.86 (s, 3H), 3.27 (ddd, *J* = 13.5, 11.2, 5.5 Hz, 1H), 2.89–2.81 (m, 1H), 2.78 (d, *J* = 6.2 Hz, 2H), 2.68 (ddd, *J* = 17.7, 11.1, 6.7 Hz, 1H), 2.43 (ddd, *J* = 17.4, 5.4, 1.8 Hz, 1H), 2.31 (s, 3H). ^{13}C NMR ($CDCl_3$) δ 148.6, 147.3, 145.7, 140.0, 134.4, 134.0, 127.2, 125.1, 121.1, 112.5, 111.1, 100.8, 96.1, 60.3, 59.4, 56.0, 55.9, 44.1, 42.3, 40.2, 23.3. HR-ESMS calcd. for $C_{21}H_{25}BrNO_5^+$ [M + H] 450.0911, found 450.0921.

9-Bromo-4-methoxy-6-methyl-5-(3,4,5-trimethoxybenzyl)-5,6,7,8-tetrahydro-[1,3]dioxolo[4,5-*g*]isoquinoline (17j). Compound **17j** was formed via Method A in 14% as a colourless oil. ^{1}H NMR ($CDCl_3$) δ 6.49 (s, 2H), 5.96 (dd, *J* = 9.0, 1.4 Hz, 2H), 4.02 (dd, *J* = 7.7, 4.5 Hz, 1H), 3.98 (s, 3H), 3.85 (s, 6H), 3.83 (s, 3H), 3.26 (ddd, *J* = 13.6, 11.2, 5.5 Hz, 1H), 2.91–2.76 (m, 3H), 2.70 (ddd, *J* = 17.7, 11.1, 5.5 Hz, 1H), 2.45 (ddd, *J* = 17.4, 5.4, 1.8 Hz, 1H), 2.35 (s, 3H). ^{13}C NMR ($CDCl_3$) δ 153.0 (× 2), 145.8, 140.0, 137.1, 136.0, 134.2, 127.2, 125.0, 106.1 (× 2), 100.9, 96.2, 61.0, 60.1, 59.4, 56.2 (× 2), 44.2, 42.4, 41.0, 23.3. HR-ESMS calcd. for $C_{22}H_{27}BrNO_6^+$ [M + H] 480.1016, found 480.0994.

General Procedure for N-Ethyl Urea Formation (compounds 18a-j). To a stirred solution of THIQ (**16**) (typically 150 mg, 1.0 eq) in MeCN (1 mL) cooled on ice, was added ethyl isocyanate (1.05 eq) and the reaction stirred for 1 h. The reaction mixture was evaporated at reduced pressure, and purified by column chromatography to give N-ethyl urea product **18**.

9-Bromo-*N*-ethyl-4-methoxy-5-phenyl-7,8-dihydro-[1,3]dioxolo[4,5-*g*]isoquinoline-6(5*H*)-carboxamide (18a). Compound **18a** was formed in 93% as a colourless foam. ^{1}H NMR ($CDCl_3$) δ 7.35–7.09 (m, 5H), 6.58 (s, 1H), 5.99 (s, 2H), 4.60 (t, *J* = 5.2 Hz, 1H), 3.81 (s, 3H), 3.59–3.51 (m,

1H), 3.35–3.26 (m, 3H), 2.86 (ddd, *J* = 15.3, 9.1, 6.0 Hz, 1H), 2.62 (dt, *J* = 16.5, 5.1 Hz, 1H), 1.14 (t, *J* = 7.2 Hz, 3H). ^{13}C NMR ($CDCl_3$) δ 157.3, 146.6, 142.2, 139.6, 135.0, 128.4, 128.3 (× 2), 127.5 (× 2), 127.2, 124.0, 101.3, 95.8, 59.6, 52.4, 38.8, 36.0, 27.5, 15.7. HR-ESMS calcd. for $C_{20}H_{22}BrN_2O_4^+$ [M + H] 433.0757, found 433.0764.

9-Bromo-*N*-ethyl-4-methoxy-5-(4-methoxyphenyl)-7,8-dihydro-[1,3]dioxolo[4,5-*g*]isoquinoline-6-*(5H)*-carboxamide (18b). Compound **18b** was formed in 71% as a colourless foam. ^{1}H NMR ($CDCl_3$) δ 7.10 (d, *J* = 8.4 Hz, 2H), 6.79 (d, *J* = 8.8 Hz, 2H), 6.49 (s, 1H), 6.00 (s, 2H), 3.82 (s, 3H), 3.77 (s, 3H), 3.59–3.49 (m, 1H), 3.36–3.26 (m, 3H), 2.86 (ddd, *J* = 15.6, 9.3, 6.1 Hz, 1H), 2.66 (dt, *J* = 16.5, 5.0 Hz, 1H), 1.15 (t, *J* = 7.2 Hz, 3H). ^{13}C NMR ($CDCl_3$) δ 158.8, 157.3, 146.6, 139.6, 135.1, 134.4, 128.7 (× 2), 128.3, 124.5, 113.7 (× 2), 101.3, 95.9, 59.7, 55.4, 52.1, 38.6, 36.0, 27.6, 15.8. HR-ESMS calcd. for $C_{21}H_{24}BrN_2O_5^+$ [M + H] 463.0863, found 463.0858.

9-Bromo-5-(2,3-dimethoxyphenyl)-*N*-ethyl-4-methoxy-7,8-dihydro-[1,3]dioxolo[4,5-*g*]isoquinoline-6-(5*H*)-carboxamide (18c). Compound **18c** was formed in 88% as a colourless solid. ^{1}H NMR ($CDCl_3$) δ 6.95–6.89 (m, 1H), 6.85 (dd, *J* = 8.2, 1.6 Hz, 1H), 6.45 (dd, *J* = 7.6, 1.6 Hz, 1H), 6.30 (t, *J* = 5.0 Hz, 1H), 6.15 (s, 1H), 5.95 (dd, *J* = 5.2, 1.3 Hz, 2H), 4.29 (ddd, *J* = 12.3, 4.9, 3.0 Hz, 1H), 4.02 (s, 3H), 3.89 (s, 3H), 3.51 (s, 3H), 3.23 (qd, *J* = 7.3, 5.1 Hz, 2H), 2.95 (ddd, *J* = 13.5, 11.4, 5.2 Hz, 1H), 2.85–2.70 (m, 2H), 1.18 (t, *J* = 7.3 Hz, 3H). ^{13}C NMR ($CDCl_3$) δ 158.0, 152.6, 146.7, 145.8, 138.8, 135.9, 135.0, 129.1, 123.8, 123.2, 120.9, 111.9, 101.3, 96.7, 60.4, 58.8, 55.9, 50.0, 35.8, 35.2, 27.6, 15.3. HR-ESMS calcd. for $C_{22}H_{26}BrN_2O_6^+$ [M + H] 493.0969, found 493.0967.

9-Bromo-5-(3,4-dimethoxyphenyl)-N-ethyl-4-methoxy-7,8-dihydro-[1,3]dioxolo[4,5-*g*]isoquinoline-6-(*5H*)-carboxamide (18d). Compound **18d** was formed in 80% as a colourless foam. ^{1}H NMR ($CDCl_3$) δ 6.89 (d, *J* = 2.0 Hz, 1H), 6.69 (d, *J* = 8.3 Hz, 1H), 6.56–6.45 (m, 2H), 5.98 (dd, *J* = 3.4, 1.4 Hz, 2H), 4.62 (t, *J* = 5.3 Hz, 1H), 3.82 (s, 3H), 3.81 (s, 3H), 3.80 (s, 3H), 3.52 (dt, *J* = 12.5, 5.2 Hz, 1H), 3.41–3.18 (m, 3H), 2.83 (ddd, *J* = 15.9, 9.5, 6.1 Hz, 1H), 2.64 (dt, *J* = 16.6, 4.8 Hz, 1H), 1.13 (t, *J* = 7.2 Hz, 3H). ^{13}C NMR ($CDCl_3$) δ 157.3, 148.9, 148.2, 146.5, 139.6,

135.0, 134.9, 128.2, 124.0, 119.5, 111.2, 110.3, 101.3, 95.9, 59.6, 56.0, 55.9, 52.1, 38.5, 35.9, 27.6, 15.7. HR-ESMS calcd for $C_{22}H_{26}BrN_2O_6^+$ [M + H] 495.0948, found 495.0955.

9-Bromo-*N*-ethyl-4-methoxy-5-(3,4,5-trimethoxyphenyl)-7,8-dihydro-[1,3]dioxolo[4,5-*g*]isoquinoline-6(5*H*)-carboxamide (18e). Compound **18e** was formed in 65% as a colourless foam. ^{1}H NMR ($CDCl_3$) δ 6.51 (s, 1H), 6.42 (s, 2H), 6.01 (dd, *J* = 7.9, 1.2 Hz, 2H), 3.86 (s, 3H), 3.80 (s, 3H), 3.77 (s, 6H), 3.50 (dd, *J* = 12.4, 6.3 Hz, 1H), 3.39 (td, *J* = 8.6, 4.5 Hz, 1H), 3.31 (q, *J* = 7.2 Hz, 2H), 2.88 (ddd, *J* = 15.0, 8.8, 6.0 Hz, 1H), 2.68 (dt, *J* = 16.5, 5.2 Hz, 1H), 1.15 (t, *J* = 7.2 Hz, 3H). ^{13}C NMR ($CDCl_3$) δ 157.3, 153.1 (× 2), 146.7, 139.6, 138.1, 136.3, 135.0, 128.4, 123.8, 104.9 (× 2), 101.4, 95.9, 60.9, 59.7, 56.4 (× 2), 52.6, 39.2, 36.0, 27.5, 15.8. HR-ESMS calcd. for $C_{23}H_{28}BrN_2O_7^+$ [M + H] 523.1074, found 523.1089.

5-Benzyl-9-bromo-*N*-ethyl-4-methoxy-7,8-dihydro-[1,3]dioxolo[4,5-*g*]isoquinoline-6(5*H*)-carboxamide (18f). Compound **18f** was formed in 62% as a pale yellow gum. ^{1}H NMR ($CDCl_3$) δ 7.34–7.20 (m, 5H), 5.97 (dd, *J* = 4.0, 1.2 Hz, 2H), 4.91 (d, *J* = 7.7 Hz, 1H), 4.34–4.23 (m, 1H), 4.08 (s, 3H), 3.42 (t, *J* = 5.2 Hz, 1H), 3.24 (ddd, *J* = 13.3, 10.4, 5.2 Hz, 1H), 3.10 (dd, *J* = 13.4, 2.9 Hz, 1H), 2.93–2.75 (m, 3H), 2.67 (ddd, *J* = 16.8, 12.8, 9.0 Hz, 2H), 0.73 (t, *J* = 7.2 Hz, 3H). ^{13}C NMR ($CDCl_3$) δ 157.7, 146.3, 139.7, 138.8, 134.4, 129.3 (× 2), 128.9 (× 2), 128.2, 126.9, 124.0, 101.1, 96.0, 59.5, 54.5, 40.4, 36.2, 35.5, 27.8, 15.1. HR-ESMS calcd. for $C_{21}H_{24}BrN_2O_4^+$ [M + H] 447.0914, found 447.0923.

9-Bromo-*N*-ethyl-4-methoxy-5-(4-methoxybenzyl)-7,8-dihydro-[1,3]dioxolo[4,5-*g*]isoquinoline-6-(5*H*)-carboxamide (18g). Compound **18g** was formed in 74% as a colourless gum. ^{1}H NMR ($CDCl_3$) δ 7.13 (d, *J* = 8.6 Hz, 2H), 6.85 (d, *J* = 8.6 Hz, 2H), 5.98 (dd, *J* = 3.8, 1.4 Hz, 2H), 4.85 (d, *J* = 7.6 Hz, 1H), 4.35–4.25 (m, 1H), 4.09 (s, 3H), 3.78 (s, 3H), 3.42 (t, *J* = 4.9 Hz, 1H), 3.22 (ddd, *J* = 13.2, 10.4, 5.2 Hz, 1H), 3.05 (dd, *J* = 13.6, 2.9 Hz, 1H), 2.98–2.60 (m, 5H), 0.76 (t, *J* = 7.2 Hz, 3H). ^{13}C NMR ($CDCl_3$) δ 158.7, 157.7, 146.4, 138.9, 134.4, 131.7, 130.3 (× 2), 128.2, 124.0, 114.3 (× 2), 101.1, 96.0, 59.6, 55.4, 54.7, 39.5, 36.2, 35.6, 27.9, 15.2. HR-ESMS calcd. for $C_{22}H_{26}BrN_2O_5^+$ [M + H] 477.1020, found 477.1018.

9-Bromo-5-(2,3-dimethoxybenzyl)-*N*-ethyl-4-methoxy-7,8-dihydro-[1,3]dioxolo[4,5-*g*]isoquinoline-6-*(5H)*-carboxamide (18h). Compound **18h** was formed in 65% as a colourless foam. ^{1}H NMR ($CDCl_3$) δ 6.96 (t, *J* = 7.9 Hz, 1H), 6.80 (dd, *J* = 8.2, 1.3 Hz, 1H), 6.67 (dd, *J* = 7.6, 1.3 Hz, 1H), 5.96 (d, *J* = 1.4 Hz, 1H), 5.96 (d, *J* = 1.4 Hz, 1H), 5.15 (dd, *J* = 9.5, 4.6 Hz, 1H), 4.43 (t, *J* = 5.3 Hz, 1H), 4.22–4.05 (m, 1H), 3.96 (s, 3H), 3.90 (s, 3H), 3.85 (s, 3H), 3.31 (ddd, *J* = 13.4, 9.6, 5.6 Hz, 1H), 3.12 (dd, *J* = 13.4, 4.7 Hz, 1H), 3.02 (ddd, *J* = 13.0, 7.2, 5.8 Hz, 1H), 2.96–2.86 (m, 2H), 2.82–2.66 (m, 2H), 0.86 (t, *J* = 7.2 Hz, 3H). ^{13}C NMR ($CDCl_3$) δ 157.6, 152.9, 147.4, 146.3, 139.1, 134.5, 132.6, 128.4, 124.5, 124.4, 123.1, 111.2, 101.1, 96.2, 60.7, 59.4, 55.8, 51.9, 36.4, 35.6, 35.5, 27.9, 15.1. HR-ESMS calcd. for $C_{23}H_{28}BrN_2O_6^+$ [M + H] 507.1125, found 507.1141.

9-Bromo-5-(3,4-dimethoxybenzyl)-*N*-ethyl-4-methoxy-7,8-dihydro-[1,3]dioxolo[4,5-*g*]isoquinoline-6(5*H*)-carboxamide (18i). Compound **18i** was formed in 66% as a pale yellow gum. ^{1}H NMR ($CDCl_3$) δ 6.81 (d, *J* = 8.1 Hz, 1H), 6.76–6.71 (m, 2H), 5.97 (dd, *J* = 4.3, 1.4 Hz, 2H), 4.93 (d, *J* = 6.8 Hz, 1H), 4.27–4.24 (m, 1H), 4.07 (s, 3H), 3.86 (s, 3H), 3.84 (s, 3H), 3.54 (t, *J* = 4.8 Hz, 1H), 3.22 (ddd, *J* = 13.1, 10.4, 5.0 Hz, 1H), 3.03 (dd, *J* = 13.6, 3.1 Hz, 1H), 2.96 (qd, *J* = 7.2, 3.6 Hz, 1H), 2.92–2.83 (m, 1H), 2.81–2.67 (m, 2H), 2.62 (ddd, *J* = 16.8, 4.8, 3.5 Hz, 1H), 0.78 (t, *J* = 7.2 Hz, 3H). ^{13}C NMR ($CDCl_3$) δ 157.7, 149.3, 148.1, 146.4, 138.9, 134.4, 132.2, 128.2, 124.0, 121.4, 112.4, 111.6, 101.1, 96.0, 59.6, 56.1 (× 2), 54.4, 40.1, 36.5, 35.6, 27.8, 15.2. HR-ESMS calcd. for $C_{23}H_{28}BrN_2O_6^+$ [M + H] 507.1125, found 507.1133.

9-Bromo-*N*-ethyl-4-methoxy-5-(3,4,5-trimethoxybenzyl)-7,8-dihydro-[1,3]dioxolo[4,5-*g*]isoquinoline-6(5*H*)-carboxamide (18j). Compound **18j** was formed in 74% as a colourless gum. ^{1}H NMR ($CDCl_3$) δ 6.41 (s, 2H), 5.96 (dd, *J* = 5.5, 1.4 Hz, 2H), 5.00 (d, *J* = 7.0 Hz, 1H), 4.19 (dd, *J* = 7.6, 4.6 Hz, 1H), 4.05 (s, 3H), 3.83 (s, 6H), 3.80 (s, 3H), 3.68 (t, *J* = 4.6 Hz, 1H), 3.22 (ddd, *J* = 13.0, 10.2, 4.9 Hz, 1H), 3.05–2.86 (m, 3H), 2.81–2.68 (m, 2H), 2.61 (dt, *J* = 8.5, 4.6 Hz, 1H), 0.83 (t, *J* = 7.2 Hz, 3H). ^{13}C NMR ($CDCl_3$) δ 157.7, 153.5 (× 2), 146.4, 138.8, 136.9, 135.4, 134.4, 128.2, 123.9, 106.1 (× 2), 101.2, 95.9, 60.9, 59.5, 56.3 (× 2), 54.0, 41.0, 36.7, 35.6, 27.8, 15.2. HR-ESMS calcd. for $C_{24}H_{30}BrN_2O_7^+$ [M + H] 537.1231, found 537.1230.

4-Bromo-11,12,14-trimethoxy-5,8,13,13a-tetrahydro-6*H*-[1,3]dioxolo[4,5-*g*]isoquinolino[3,2-*a*]isoquinoline (19). Compound **19** was formed from **16h** via Method B in 47% as a brown oil. ^{1}H NMR ($CDCl_3$) δ 6.85 – 6.71 (m, 2H), 6.00 (d, *J* = 1.4 Hz, 1H), 5.98 (d, *J* = 1.4 Hz, 1H), 4.17–4.10 (m, 1H), 4.04 (dd, *J* = 11.1, 4.3 Hz, 1H), 4.00 (s, 3H), 3.89 (d, *J* = 15.6 Hz, 1H), 3.84 (s, 3H), 3.78 (s, 3H), 3.42 (dd, *J* = 17.4, 3.6 Hz, 1H), 3.06 (dt, *J* = 11.6, 6.0 Hz, 1H), 2.87–2.79 (m, 2H), 2.66 (dt, *J* = 11.3, 5.6 Hz, 1H), 2.52 (dd, *J* = 17.4, 11.1 Hz, 1H). ^{13}C NMR ($CDCl_3$) δ 151.0, 146.6, 145.9, 139.8, 135.0, 129.1, 127.9, 127.0, 126.3, 121.8, 110.7, 101.2, 96.5, 60.1, 59.6, 57.0, 56.0, 54.3, 46.5, 30.1, 26.6. HR-ESMS calcd. for $C_{21}H_{23}BrNO_5^+$ [M + H] 448.0754, found 448.0759.

Pharmacology. *Compound preparation and storage*. A 10^{-2} M stock solution was prepared for each compound by dissolving the compound in sterile-filtered DMSO (Sigma D2650), and the solution was stored at –20 °C until use.

Cell culture and reagents. The human breast cancer cell line MCF-7^{WT} (HTB-22) and pancreatic cancer cell line PANC-1 (CRL-1469) were purchased directly from American Type Culture Collection (ATCC) and cultured in minimum essential medium alpha (MEMα) (Invitrogen 32561-037) and Dulbecco's modified eagle medium (DMEM) (Invitrogen 10566-016), respectively. In addition, each culture medium was supplemented with 10% foetal bovine serum (FBS) (Invitrogen 10100-147). The doxorubicin-selected P-gp expressing variant NCI/Adr^{Res} cell line was obtained from Dr K Cowan (National Cancer Institute, Bethesda, MD).[37] The NCI/Adr^{RES} cell line was cultured in DMEM supplemented with 10% foetal calf serum (FCS) and penicillin/streptomycin, with every third passage supplemented with 3 μM doxorubicin to maintain selection pressure. Cells were maintained at 37 °C in a humidified atmosphere containing 5% CO_2. Before use, cell lines were tested for the presence of mycoplasma by using a MycoAlert Mycoplasma detection kit (Lonza LT07-318) according to the manufacturer's instructions; cells employed in the assays tested negative for mycoplasma.

Cell-cycle assay. Cells were detached by 0.05% trypsin-EDTA (Invitrogen 15400-054) and seeded at 2×10^4 cells per well in 24-well plates 48 h before treatment. Cells were then treated with vehicle control, noscapine analogues at 10 μM, vincristine, noscapine (reference controls) at 100 nM and 10 μM, respectively, or vehicle control for 18 h before detachment by 0.05% trypsin-EDTA. Following deactivation of trypsin, cells were stained with Hoechst 33342 working solution (10 mg/mL) (Invitrogen H3570) for 60 min. The different stages of the cell proliferation cycle were detected by a FACSCanto II fluorescence-activated cell sorting (FACS) analyser (BD Biosciences, Australia) using the Pacific blue channel (450 nm). The amount of cells present at G1, S and G2/M phases of the cell cycle were obtained as percentage values following data processing with FlowJo flow cytometry analysis software v10. The percentage increase in arrested cells by noscapine analogues were calculated with reference to the percentage of cells at the G2/M phase in the vehicle control using the following formula: [(%cells in G2/M (noscapine analogues) – (%cells in G2/M (vehicle control))/(%cells in G2/M (vehicle control)) x 100%.

Tubulin polymerisation assay. Tubulin polymerisation was recorded turbidimetrically at 340 nm in PerkinElmer EnVision2101 Multilabel Reader equipped with temperature controllers. Compounds of interest (2 mM in sterile-filtered DMSO) were dissolved in General Tubulin Buffer (80 mM PIPES pH 6.9, 2 mM $MgCl_2$, 0.5 mM EGTA) to a final concentration of 10 μM and were added to 96-half area well plate and kept at 37 °C. Tubulin was dissolved to a final concentration of 3 mg/mL in 80 mM PIPES pH 6.9, 0.5 mM $MgCl_2$, 0.5 mM EGTA, 1 mM GTP, 10.2% glycerol and was kept at 4 °C prior to addition to plate. Kinetic absorbance reading started immediately following addition of tubulin to the plate, and was recorded at 37 °C over a period of 60 min. The tubulin polymerisation assay kit (BK006P) used to conduct this study was supplied by Cytoskeleton Inc.

Cell cytotoxicity assay. Cells were detached using 0.25% trypsin and seeded at 1500 cells per well in flat-bottomed 96-well plates overnight before treatment. Cells were then treated with various concentrations of vinblastine (reference control) or noscapine analogues for 6 d. The count of viable

cells was determined using a standard MTT assay for cell cytotoxicity. The absorbance in each well was measured using iMARK 96-well plate reader at 570 nm. All absorbance values were corrected by subtracting background absorbance. The absorbance value in the control well was assigned a value of 100%, and absorbances were normalised to this value. The proportion of viable cells was plotted as a function of noscapine analogues concentration, and the EC_{50} value to effect cell death was estimated from the resultant dose-response curve.

Combination cytotoxicity assays. For combination cytotoxicity assays, cells were incubated with vinblastine as described above either in the presence of absence of **18g** (0.1–3 μM). The nature of interaction between drugs co-administered in cytotoxicity assays was evaluated using Combination Indices (CI) that were derived from the *Lowe's Additivity Model*;[38]

$$Combination\ Index = \frac{d_1}{(D_x)1} + \frac{d_2}{(D_x)2}$$

where d_1 and d_2 are the concentrations of drug needed respectively to inhibit x% of cells when used as a combination, $(D_x)_1$ is the concentration of drug 1 required to inhibit x% of cells, $(D_x)_2$ is the concentration of drug 2 needed to inhibit x% of cells. The indices were calculated using concentrations interpolated where the x% cells affected was 50% (IC_{75}) for vinblastine in combination with **18g**. A CI value = 1 indicates an additive effect, CI<1 indicates synergy and CI>1 indicates antagonism. It was not possible to calculate combination values where the combination resulted in a cell viability of less than 20%.

Purification and functional assessment of P-gp. P-gp was expressed in *Trichoplusia ni* (High-Five) cells following infection with recombinant baculovirus containing the specific mutant isoform as previously described.[32] P-gp was purified from High-Five cell membranes using immobilised metal affinity chromatography (IMAC) in a gravity based system, according to previously published methods with some modifications.[32,33] In particular, the crude membranes (30-100 mg) were suspended (5 mg mL^{-1} protein) in solubilisation buffer supplemented with a 0.4% (w/v) lipid mixture (4:1 ratio of *E coli* extract:cholesterol) and 2% (w/v) dodecyl-β-D-maltoside (DDM).

ATPase activity of P-gp. Functional assessment of P-gp was achieved by measuring its ATPase activity based on the rate of inorganic phosphate liberation by P-gp containing proteoliposomes using a modified colorimetric assay.[33,39] In order to investigate the stimulation of ATP hydrolysis, the activity was measured as a function of added drug concentration. Proteoliposomes (0.1-0.5 μg) were incubated with ATP (2 mM) and various drug concentrations (10^{-9} to 10^{-4} M) for 40 min at 37 °C in 96-well plates. In all cases the activity was expressed as moles of P_i liberated per unit time for a unit of purified P-gp. The potency (EC_{50}) and extent of stimulation of ATPase activity (v) were estimated by non-linear regression of the general dose-response relationship to plots of activity as a function of drug concentration ([D]): $v = v_{initial} + \left(v_{final} - v_{initial}\right)/\left(1 + 10^{\left(log10(EC_{50} - [D])\right)}\right)$, where [D] is the drug concentration, $v_{initial}$ is the activity in the absence of drug and v_{final} is the maximal activity observed.

Calcein-AM accumulation assay in intact cells. The calcein-AM assay to measure the transport function of P-gp was based on previously published methods.[31,40] MCF-7^{WT} and NCI/Adr^{RES} cells were seeded into 96-well tissue culture plates at a density of 2×10^3 cells per well in 100 μL and allowed to adhere for 2 d at 37 °C with 5% CO_2. Following incubation, the medium was aspirated and cells were washed with PBS and re-suspended in 100 μL Hank's Buffered Salt Solution (HBSS). Test compounds (100 μL) were added at a 2X final concentration in HBSS from an original stock solution of 50 mM in DMSO. The final solvent (DMSO) concentration in the wells did not exceed 1% (v/v). Calcein-AM was added from a 100X HBBS stock to give a final concentration of 1 μM. The intracellular calcein accumulation (i.e. fluorescence intensity) was plotted as a function of time and analysed by linear regression using GraphPad Prism® Software v6. The slope of each line was used to determine the rate of calcein accumulation.

■ ASSOCIATED CONTENT

Supporting Information

The Supporting Information is available free of charge on the ACS Publications website:

Scheme and synthesis of **13**

Dose-response curves of **5** and **18g** against sensitive and resistant cell lines

FACS analysis against PANC-1 (for **17g**) and against MCF-7 cells (for **17g** and **18g**)

NMR spectra of **17g** and **18g**

Molecular formula strings

■ AUTHOR INFORMATION

Corresponding Author

*For P.J.S.: phone: +613 9903 9542; E-mail: peter.scammells@monash.edu.

ORCID

Shane M. Devine: 0000-0001-8727-7392

Peter J. Scammells: 0000-0003-2930-895X

Ben Capuano: 0000-0001-5434-0180

Author Contributions

The manuscript was written through contributions of all authors, and all authors have given approval to the final version of the manuscript.

Notes

The authors declare no competing financial interest.

■ ACKNOWLEDGEMENTS

The authors would like to thank Sun Pharmaceutical Industries for their kind donation of noscapine.

■ ABBREVIATIONS USED

CI, combination indices; FACS, fluorescence-activated cell sorting; P-gp, P-glycoprotein; SAR, structure-activity relationship; TDI, tubulin-depolymerisation inhibitors, THIQ, tetrahydroisoquinoline; TPI, tubulin-polymerisation inhibitors;

■ REFERENCES

(1) Segal, M. S.; Goldstein, M. M.; Attinger, E. O. The Use of Noscapine (Narcotine) as an Antitussive Agent. *Chest* **1957**, *32* (3), 305–309.

(2) Empey, D. W.; Laitinen, L. A.; Young, G. A.; Bye, C. E.; Hughes, D. T. D. Comparison of the Antitussive Effects of Codeine Phosphate 20 Mg, Dextromethorphan 30 Mg and Noscapine 30 Mg Using Citric Acid-Induced Cough in Normal Subjects. *Eur. J. Clin. Pharmacol.* **1979**, *16* (6), 393–397.

(3) Dahlström, B.; Mellstrand, T.; Löfdahl, C. G.; Johansson, M. Pharmakokinetic Properties of Noscapine. *Eur. J. Clin. Pharmacol.* **1982**, *22* (6), 535–539.

(4) Karlsson, M. O.; Dahlström, B.; Eckernäs, S. Å.; Johansson, M.; Alm, A. T. Pharmacokinetics of Oral Noscapine. *Eur. J. Clin. Pharmacol.* **1990**, *39* (3), 275–279.

(5) Ye, K.; Ke, Y.; Keshava, N.; Shanks, J.; Kapp, J. A.; Tekmal, R. R.; Petros, J.; Joshi, H. C. Opium Alkaloid Noscapine Is an Antitumor Agent That Arrests Metaphase and Induces Apoptosis in Dividing Cells. *Proc. Natl. Acad. Sci. U.S.A.* **1998**, *95* (4), 1601–1606.

(6) Alisaraie, L.; Tuszynski, J. A. Determination of Noscapine's Localization and Interaction with the Tubulin-A/B Heterodimer. *Chem. Biol. Drug Des.* **2011**, *78* (4), 535–546.

(7) Naik, P. K.; Santoshi, S.; Rai, A.; Joshi, H. C. Molecular Modelling and Competition Binding Study of Br-Noscapine and Colchicine Provide Insight Into Noscapinoid-Tubulin Binding Site. *J. Mol. Graph. Model.* **2011**, *29* (7), 947–955.

(8) Karna, P.; Rida, P. C. G.; Pannu, V.; Gupta, K. K.; Dalton, W. B.; Joshi, H.; Yang, V. W.; Zhou, J.; Aneja, R. A Novel Microtubule-Modulating Noscapinoid Triggers Apoptosis by Inducing

Spindle Multipolarity via Centrosome Amplification and Declustering. *Cell Death Differ.* **2011**, *18* (4), 632–644.

(9) Mourey, R. J.; Dawson, T. M.; Barrow, R. K.; Enna, A. E.; Snyder, S. H. [3H]Noscapine Binding Sites in Brain: Relationship to Indoleamines and the Phosphoinositide and Adenylyl Cyclase Messenger Systems. *Mol. Pharmacol.* **1992**, *42* (4), 619–626.

(10) Karlsson, M. O.; Dahlström, B.; Neil, A. Characterization of High-Affinity Binding Sites for the Antitussive [3H]Noscapine in Guinea Pig Brain Tissue. *Eur. J. Pharmacol.* **1988**, *145* (2), 195–203.

(11) Doddapaneni, R.; Patel, K.; Chowdhury, N.; Singh, M. Reversal of Drug-Resistance by Noscapine Chemo-Sensitization in Docetaxel Resistant Triple Negative Breast Cancer. *Sci. Rep.* **2017**, *7* (1), 15824.

(12) Ghaly, P. E.; Abou El-Magd, R. M.; Churchill, C. D. M.; Tuszynski, J. A.; West, F. G. A New Antiproliferative Noscapine Analogue: Chemical Synthesis and Biological Evaluation. *Oncotarget* **2016**, *7* (26), 40518–40530.

(13) Ghaly, P. E.; Churchill, C. D. M.; Abou El-Magd, R. M.; Hájková, Z.; Dráber, P.; West, F. G.; Tuszynski, J. A. Synthesis and Biological Evaluation of Structurally Simplified Noscapine Analogues as Microtubule Binding Agents. *Can. J. Chem.* **2017**, *95* (6), 649–655.

(14) Tian, X.; Liu, M.; Zhu, Q.; Tan, J.; Liu, W.; Wang, Y.; Chen, W.; Zou, Y.; Cai, Y.; Han, Z.; Huang, X. Down-Regulation of Liver-Intestine Cadherin Enhances Noscapine-Induced Apoptosis in Human Colon Cancer Cells. *Expert Rev Anticancer Ther* **2017**, *17* (9), 857–863.

(15) Pradhan, S.; Mahaddalkar, T.; Choudhary, S.; Manhcukonda, N.; Nagireddy, P. R.; Kantevari, S.; Lopus, M. Elucidation of the Tubulin-Targeted Mechanism of Action of 9-(3-Pyridyl) Noscapine. *Curr. Top. Med. Chem.* **2017**, *17* (22), 2569–2574.

(16) Tomar, V.; Kukreti, S.; Prakash, S.; Madan, J.; Chandra, R. Noscapine and Its Analogs as Chemotherapeutic Agent: Current Updates. *Curr. Top. Med. Chem.* **2017**, *17* (2), 174–188.

(17) Mahaddalkar, T.; Manchukonda, N.; Choudhary, S.; Cheriyamundath, S.; Mohanpuria, N.; Kantevari, S.; Lopus, M. Subtle Alterations in Microtubule Assembly Dynamics by Br□TMB□

Noscapine Strongly Suppress Triple□Negative Breast Cancer Cell Viability Without Mitotic Arrest. *ChemistrySelect* **2016**, *1* (14), 4313–4319.

(18) Xu, G.; Niu, Z.; Dong, J.; Zhao, Y.; Zhang, Y.; Li, X. Noscapine Inhibits Human Hepatocellular Carcinoma Growth Through Inducing Apoptosis in Vitro and in Vivo. *Neoplasma* **2016**, *63* (5), 726–733.

(19) Debono, A.; Capuano, B.; Scammells, P. J. Progress Toward the Development of Noscapine and Derivatives as Anticancer Agents. *J. Med. Chem.* **2015**, *58* (15), 5699–5727.

(20) Aneja, R.; Vangapandu, S. N.; Joshi, H. C. Synthesis and Biological Evaluation of a Cyclic Ether Fluorinated Noscapine Analog. *Bioorg. Med. Chem.* **2006**, *14* (24), 8352–8358.

(21) Anderson, J. T.; Ting, A. E.; Boozer, S.; Brunden, K. R.; Danzig, J.; Dent, T.; Harrington, J. J.; Murphy, S. M.; Perry, R.; Raber, A.; Rundlett, S. E.; Wang, J.; Wang, N.; Bennani, Y. L. Discovery of S-Phase Arresting Agents Derived From Noscapine. *J. Med. Chem.* **2005**, *48* (8), 2756–2758.

(22) Anderson, J. T.; Ting, A. E.; Boozer, S.; Brunden, K. R.; Crumrine, C.; Danzig, J.; Dent, T.; Faga, L.; Harrington, J. J.; Hodnick, W. F.; Murphy, S. M.; Pawlowski, G.; Perry, R.; Raber, A.; Rundlett, S. E.; Stricker-Krongrad, A.; Wang, J.; Bennani, Y. L. Identification of Novel and Improved Antimitotic Agents Derived From Noscapine. *J. Med. Chem.* **2005**, *48* (23), 7096–7098.

(23) Bennani, Y. L.; Gu, W.; Canales, A.; Díaz, F. J.; Eustace, B. K.; Hoover, R. R.; Jiménez-Barbero, J.; Nezami, A.; Wang, T. Tubulin Binding, Protein-Bound Conformation in Solution, and Antimitotic Cellular Profiling of Noscapine and Its Derivatives. *J. Med. Chem.* **2012**, *55* (5), 1920–1925.

(24) DeBono, A. J.; Xie, J. H.; Ventura, S.; Pouton, C. W.; Capuano, B.; Scammells, P. J. Synthesis and Biological Evaluation of N-Substituted Noscapine Analogues. *ChemMedChem* **2012**, *7* (12), 2122–2133.

(25) DeBono, A. J.; Mistry, S. J.; Xie, J.; Muthiah, D.; Phillips, J.; Ventura, S.; Callaghan, R.; Pouton, C. W.; Capuano, B.; Scammells, P. J. The Synthesis and Biological Evaluation of Multifunctionalised Derivatives of Noscapine as Cytotoxic Agents. *ChemMedChem* **2014**, *9* (2),

399–410.

(26) Zimmermann, T. J.; Roy, S.; Martinez, N. E.; Ziegler, S.; Hedberg, C.; Waldmann, H. Biology-Oriented Synthesis of a Tetrahydroisoquinoline-Based Compound Collection Targeting Microtubule Polymerization. *ChemBioChem* **2013**, *14* (3), 295–300.

(27) Bischler, A.; Napieralski, B. Zur Kenntniss Einer Neuen Isochinolinsynthese. *Ber. Dtsch. Chem. Ges.* **1893**, *26* (2), 1903–1908.

(28) Guy, M.; Freeman, S.; Alder, J. F.; Brandt, S. D. The Henry Reaction: Spectroscopic Studies of Nitrile and Hydroxylamine by-Products Formed During Synthesis of Psychoactive Phenylalkylamines. *Cent. Eur. J. Chem.* **2008**, *6* (4), 526–534.

(29) Sun, H.; Zhu, L.; Yang, H.; Qian, W.; Guo, L.; Zhou, S.; Gao, B.; Li, Z.; Zhou, Y.; Jiang, H.; Chen, K.; Zhen, X.; Liu, H. Asymmetric Total Synthesis and Identification of Tetrahydroprotoberberine Derivatives as New Antipsychotic Agents Possessing a Dopamine D(1), D(2) and Serotonin 5-HT(1A) Multi-Action Profile. *Bioorg. Med. Chem.* **2013**, *21* (4), 856–868.

(30) Hamel, E. Evaluation of Antimitotic Agents by Quantitative Comparisons of Their Effects on the Polymerization of Purified Tubulin. *Cell Biochem. Biophys.* **2003**, *38* (1), 1–21.

(31) Homolya, L.; Holló, Z.; Germann, U. A.; Pastan, I.; Gottesman, M. M.; Sarkadi, B. Fluorescent Cellular Indicators Are Extruded by the Multidrug Resistance Protein. *J. Biol. Chem.* **1993**, *268* (29), 21493–21496.

(32) Taylor, A. M.; Storm, J.; Soceneantu, L.; Linton, K. J.; Gabriel, M.; Martin, C.; Woodhouse, J.; Blott, E.; Higgins, C. F.; Callaghan, R. Detailed Characterization of Cysteine-Less P-Glycoprotein Reveals Subtle Pharmacological Differences in Function From Wild-Type Protein. *Br. J. Pharmacol.* **2001**, *134* (8), 1609–1618.

(33) Crowley, E.; O'Mara, M. L.; Reynolds, C.; Tieleman, D. P.; Storm, J.; Kerr, I. D.; Callaghan, R. Transmembrane Helix 12 Modulates Progression of the ATP Catalytic Cycle in ABCB1. *Biochemistry* **2009**, *48* (26), 6249–6258.

(34) Merlin, J. L. Concepts of Synergism and Antagonism. *Anticancer Res.* **1994**, *14* (6A), 2315–2319.

(35) Gottlieb, H. E.; Kotlyar, V.; Nudelman, A. NMR Chemical Shifts of Common Laboratory Solvents as Trace Impurities. *J. Org. Chem.* **1997**, *62* (21), 7512–7515.

(36) Carrera, G. M.; Garvey, D. S. Synthesis of Novel Substituted Spirohydantoins. *J. Heterocyclic Chem.* **1992**, *29* (4), 847–850.

(37) Mehta, K.; Devarajan, E.; Chen, J.; Multani, A.; Pathak, S. Multidrug-Resistant MCF-7 Cells: an Identity Crisis? *J. Natl. Cancer Inst.* **2002**, *94* (21), 1652–1654.

(38) Chou, T.-C. Theoretical Basis, Experimental Design, and Computerized Simulation of Synergism and Antagonism in Drug Combination Studies. *Pharmacol. Rev.* **2006**, *58* (3), 621–681.

(39) Chifflet, S.; Torriglia, A.; Chiesa, R.; Tolosa, S. A Method for the Determination of Inorganic Phosphate in the Presence of Labile Organic Phosphate and High Concentrations of Protein: Application to Lens ATPases. *Anal. Biochem.* **1988**, *168* (1), 1–4.

(40) Muthiah, D.; Callaghan, R. Dual Effects of the PI3K Inhibitor ZSTK474 on Multidrug Efflux Pumps in Resistant Cancer Cells. *Eur. J. Pharmacol.* **2017**, *815*, 127–137.

TOC Graphic